The Dissertation Committee for Stephanie Michelle Moya Certifies that this is the approved version of the following dissertation:

RADIOSENSITIZING EFFECTS OF THROMBIN PEPTIDE TP508 ON MEDULLOBLASTOMA CANCER STEM CELLS

Committee:

Darrell H. Carney, Ph.D., Mentor

Tracy Toliver-Kinsky, Ph.D.

Gerald Fuller, Ph.D.

Sandra Hatch, M.D.

Tapas Hazra, Ph.D.

David Niesel, Ph.D.

Dean, Graduate School

RADIOSENSITIZING EFFECTS OF THROMBIN PEPTIDE TP508 ON MEDULLOBLASTOMA CANCER STEM CELLS

by

Stephanie Michelle Moya, B.S.

Dissertation

Presented to the Faculty of the Graduate School of

The University of Texas Medical Branch

in Partial Fulfillment

of the Requirements

for the Degree of

Doctor of Philosophy

The University of Texas Medical Branch

March, 2017

DEDICATION

To my family for always believing in me.

ACKNOWLEDGEMENTS

I would first like to thank my mentor, Dr. Darrell Carney, for his constant support and guidance throughout my years at UTMB. Thank you for accepting me as a student in your lab and for allowing me to work on such an exciting project.

A most special and heartfelt thank you to Dr. Carla Kantara for training me and offering me invaluable advice and guidance these past five years. Without her support and mentoring I would not have become the scientist that I am today. I will always be grateful to her for motivating me to strive for excellence and for being a role model not only to me but also to many other graduate students at UTMB.

I would like to thank Dr. Gerald Fuller for pushing me to think critically and for offering insight on my new findings. I would also like to extend my appreciation to Dr. Toliver-Kinsky for her support, first as the BMB program director, and also as my committee chair. I also owe a big thank you to Dr. Tapas Hazra and Dr. Sandra Hatch for agreeing to serve as my committee members and for offering valuable feedback and advice regarding my project.

I would also like to thank Dr. Laurie Sower for her help in keeping our laboratory studies running smoothly and making sure we were all on track. To current and past lab members, Kempaiah Rayavara, Weihua Cui, and Aaron Cherry, I would like to thank them for their friendship and willingness to assist me with animal experiments.

I would also like to give a big thank you to Dr. Bradford Loucas for continuously being willing to help with irradiation of my cells. Without him operating the cesium irradiator none of these studies would have been possible. I am also grateful to Kenneth Escobar at the UTMB histopathology core for processing the neurospheres for staining.

In the graduate school, I would like to thank Dr. David Niesel for his support throughout my graduate years and for believing in me since my year as a PREP student. I also greatly appreciate Dr. James Lee for his support as program director and for being an amazing student advocate.

In the administrative offices, I would like to thank JoAlice Whitehurst and Laura Teed for helping me when I had questions regarding classes or graduation requirements. A special thank you to Claiborne Fant, for her continual support with the Committee for Career Development.

Last but certainly not least, I am grateful for the love and encouragement from my family, fiancé, and friends that kept me going from start to finish!

Radiosensitizing Effects of Thrombin Peptide TP508 on Medulloblastoma Cancer Stem Cells

Publication No._____

Stephanie Michelle Moya, Ph.D.

The University of Texas Medical Branch, 2017

Supervisor: Darrell H. Carney

Brain cancer is the second leading cause of cancer-related deaths in children in the United States, with medulloblastoma leading all pediatric cases. With intensive treatments, including surgery, radiation, and/or chemotherapy, the average 5-year survival rate is approximately 60-80 percent. Unfortunately, nearly all survivors experience hindered quality of life due to radiation therapy (RT) induced cognitive dysfunctions. Additionally, current therapies are unsuccessful in completely eradicating the disease due to their inability to target a subpopulation of resistant cancer stem cells (CSCs) known to be responsible for tumor recurrence. Therefore, it is important to develop novel non-toxic therapeutics capable of sparing normal cells/tissues to prevent cognitive dysfunctions, while also sensitizing CSCs to radiation therapy (RT) in order to prevent tumor relapse.

Recently our laboratory showed that thrombin peptide TP508, a novel 23-amino acid investigational drug, protects normal neural stem cells from ionizing radiation damage. To determine whether the peptide would also protect brain CSCs from radiation damage, I examined the effects of TP508 on the stemness and tumor relapse potential of medulloblastoma and glioblastoma CSCs, post-RT. In both tumor types, I concluded that TP508 did not protect CSCs from RT.

More specifically, in medulloblastoma, I found that TP508 decreased CSC viability and stemness potential *in vitro* and delayed tumor growth *in vivo* post-RT. Therefore, I concluded that TP508 acts as a radiosensitizer of CSCs, making them more susceptible to RT damage and cellular death.

Based on these findings, my goal was to identify the mechanisms by which the peptide exerts its radiosensitizing effects on CSCs. Specifically, my studies focused on investigating the effects of TP508 on DNA double-strand break repair mechanisms. Results showed that TP508 significantly sensitizes medulloblastoma CSCs to RT by inhibiting activation of DNA repair molecule, p-BRCA1, involved in homologous recombination, and by downregulating the activation of checkpoint kinases necessary for cell cycle arrest and repair.

A strong understanding of the mechanisms by which TP508 exerts its effects on CSCs will allow for the development of this peptide as a novel therapeutic to target brain cancers, improve clinical outcome, and prevent tumor relapse.

TABLE OF CONTENTS

LIST OF TABLES

LIST OF FIGURES

LIST OF ABBREVIATIONS

CD44	Cluster of differentiation 44
CD133	Cluster of differentiation 133
Chk1	Checkpoint kinase 1
Chk2	Checkpoint kinase 2
CNS	Central nervous system
CSC	Cancer stem cell
DRR	DNA repair response
DSB	Double Strand Break
EGL	External granule layer
Exp	Experiment
Fig	Figure
γH2AX	gamma-H2A histone family, member X
GNP	Granule neuron precursors
H&E	Hematoxylin and eosin
HR	Homologous recombination
Hr(s)	Hour(s)
IF	Immunofluorescence
IGL	Internal granule layer
LGR5	Leucine-rich repeat containing G protein-coupled receptor 5
MRN	Mre11-Rad50-NBS1
NHEJ	Non-homologous end joining

PCNA	Proliferating cell nuclear antigen
RT	Radiation therapy
Shh	Sonic Hedgehog
SSB	Single strand breaks
TP508	Thrombin peptide 508
vs	Versus
WT	Wild-type
WB	Western blot

PATENT SUBMISSION

Some figures and material presented in this dissertation has been submitted to filed US Patent #20150359855, "METHODS OF USING THROMBIN DERIVATIVES TO TREAT MEDULLOBLASTOMA" Authors: D. Carney, C. Kantara, S. Moya[2]

CHAPTER 1: INTRODUCTION

1.1 Brain Cancer Types

1.1.1 Medulloblastoma

Cancer is characterized by an uncontrolled and abnormal cellular growth that can potentially lead to tissue damage, metastasis, and death. According to the 2016 American Cancer Society Cancer Facts and Figures, 1 in 4 deaths in the United States are caused by cancer[3]. In children, brain cancer is the second leading cause of cancer-related deaths, with approximately 5000 new cases each year[3]. More specifically, medulloblastoma is the most common malignant brain tumor in children, accounting for 25–30 percent of primary central nervous system (CNS) tumors[3, 4].

Medulloblastoma is a grade IV primary brain tumor that develops in the cerebellum[5]. Due to its wide variability in molecular, histological, and clinical profiles, medulloblastoma has been classified into 4 unique molecular profiles (Fig 1.1). In 2012, an international consensus was reached in naming the four groups, Sonic hedgehog (Shh), Wingless (Wnt), Group C, and Group D[6, 7]. The Shh and Wnt groups are named according to the regulating pathways that cause their respective subtype, while the specific driver mutations for groups C and D remain unknown. Although medulloblastoma is most commonly diagnosed in children, the age distribution of patients can vary from less than 1-year to 36 years of age. Histopathological profiles amongst the four groups include classic, large cell/anaplastic, and desmoplastic nodular. The 5-year overall survival rates range from 32-94 percent, with group C having the worst prognosis due to poor cellular differentiation being associated with poor clinical outcome[8]. The poor prognosis in patients

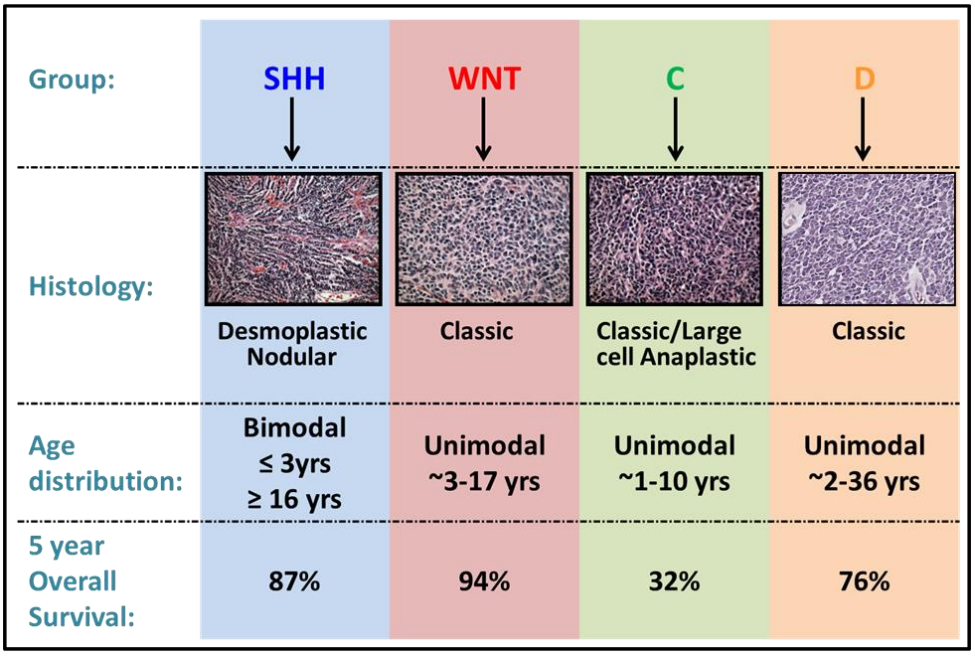

Figure 1.1: Medulloblastoma Subtypes

with group C medulloblastoma is attributed to its classic/large cell anaplastic histology being less differentiated and therefore more resistant to therapeutic treatments[8].

Both the Wnt and Shh pathways have been implicated in promoting the development of medulloblastoma during embryogenesis; targeting these specific signaling molecules have been shown to reduce tumor growth *in vivo*[9-12]. During embryogenesis the cerebellum is formed by progenitor and stem cells located in the ventricular zone and upper rhombic lip of the fourth ventricle of the brain. These progenitor cells form an external and internal granule layer (EGL and IGL) which begin to shape the cerebellum. During normal cerebellar development, Shh signals the proliferation of granule neuron precursors (GNPs) in the EGL which exit the cell cycle and migrate into the IGL where they differentiate into mature granule neurons[13]. It is believed that through dysregulation of Shh inhibitors or upregulation of Shh secretion there is an uncontrolled proliferation of GNPs which fail to

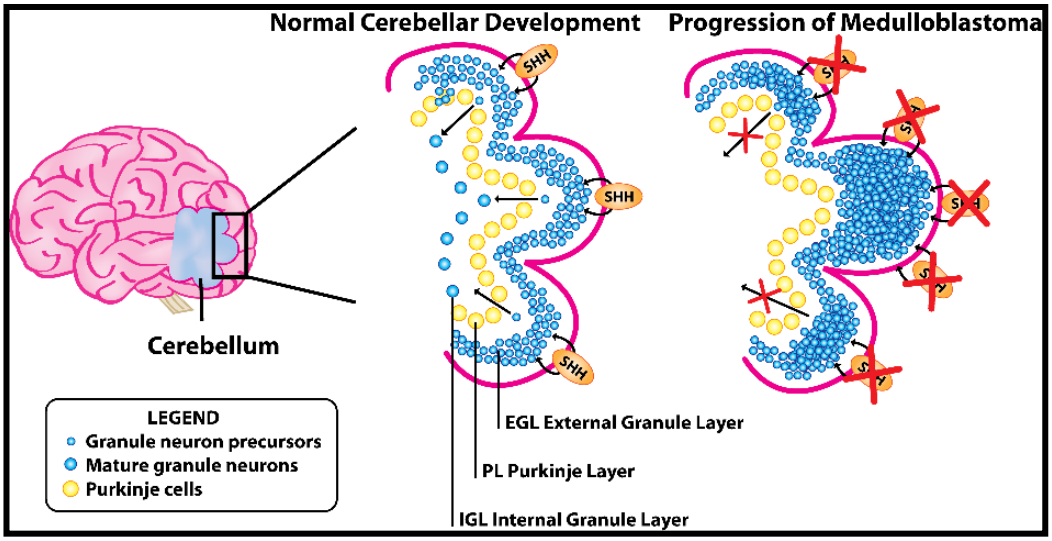

Figure 1.2: Role of Shh in Medulloblastoma Development

migrate and instead form a tumorous mass in the EGL, hence giving rise to a medulloblastoma (Fig 1.2)[5, 13].

Activation of the canonical Wnt signaling pathway also plays an important role in regulating neural stem cell proliferation and development of the cerebellum. However, the Wnt subtype medulloblastoma is believed to originate from progenitor cells in the hindbrain located in the lower rhombic lip rather than the upper rhombic lip[13].

It is important to note that regardless of the specific signaling pathway involved, the underlying cause of medulloblastoma seems to be dysregulation of normal stem and progenitor cells during development. As such, aberrant regulation of normal stem cells is believed to be the culprit in the initiation and tumor progression of medulloblastoma. It is hypothesized that when normal stem cells lose their homeostatic proliferative functions they develop a mutated phenotype and transform into cancer stem cells (CSCs)[14]. Therefore, targeting CSCs and the pathways by which they are regulated is crucial to effectively treat and eradicate the tumors.

1.1.2 Medulloblastoma Treatment Options

Current available treatment protocols for medulloblastoma include surgical removal of the tumor, fractionated radiation therapy (RT), and intensive chemotherapy treatments[15, 16]. Depending on the severity of the case, the first line of treatment is sometimes the placement of a cerebrospinal fluid shunt to reduce intracranial pressure. This is followed by surgical removal of the tumor with the goal to excise as much of the tumor as possible without damaging surrounding healthy tissue. Analysis of the biopsied tumor can then help determine the medulloblastoma subtype and allow for a subtype-specific treatment plan[17-20].

Following surgical resection of the tumor, radiation treatment is administered in two phases. Patients first receive a 23.4Gy total dose to the entire brain and spinal cord administered in 1.8Gy fractionated sessions. This is followed by a higher 30.6Gy total radiation dose directly targeted at the tumor, also in 1.8Gy fractionated sessions, for a total radiation dose of 54Gy[21]. Radiation treatment is not recommended for patients less than 3 years of age due to the severe adverse side effects it can have on the immature/undeveloped nervous system. In order to determine the optimal care for each patient, risk stratifications are examined in which the age, extent of tumor resection, and metastatic stage are all taken into consideration. For example, evidence of metastasis and/or residual tumor larger than $1.5cm^2$ places patients in a high-risk treatment protocol, in which they receive a 36-36.9Gy dose to the brain and spinal cord (vs 23.4Gy)[22].

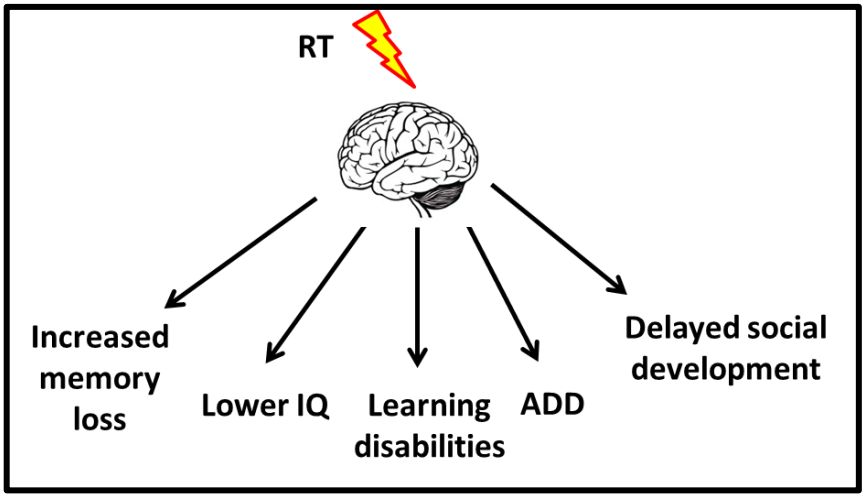

Figure 1.3: Radiation-Induced Cognitive Deficits

In most treatment plans, chemotherapy is additionally recommended to reduce the chances of tumor recurrence[23]. Chemotherapeutic agents, include vincristine, carboplatin, and cyclophosphamide. A combination of these agents can be used simultaneously with RT for a more aggressive approach in patients who cannot undergo surgical removal of the tumor. Standard-risk patients receive chemotherapy treaments weekly in combination with radiation therapy, and then continue chemotherapy treatments after completion of RT[24].

Although these rigorous treatment plans yield a promising average 5-year survival rate of 60-80 percent[25], nearly all survivors experience hindered quality of life and long-term cognitive deficits due to the tri-modality of care, particularly in regards to radiation therapy[26]. Radiation therapy in particular can induce various cognitive deficits, including increased memory loss, lower IQ, learning disabilities, attention deficit disorder and delayed social and behavioral development[21, 27-30] (Fig 1.3). Patients often require additional and continual medical care to address these issues.

After completing therapeutic treatment, patients are monitored periodically to follow-up with potential long-term treatment complications and monitor recurrence of the disease. Unfortunately, recurrence of the tumor occurs in approximately 20-30 percent of patients post-treatment, accompanied with a low 5-year survival rate of less than 5

percent[31-33]. Recurrence of the disease is believed to be caused by RT resistant cancer stem cells within the tumor bulk that are capable of repopulating the tumor. Therefore, there is a need to develop novel treatment options that can both decrease central nervous system toxicity and target cancer stem cells to prevent tumor recurrence[17].

1.1.3 Glioblastoma

Glioblastoma is the most common and most lethal malignant primary brain tumor in adults[34]. Upon diagnosis, median patient survival is 14.6 months with treatment, and 3-4 months without treatment[35]. Similarly to medulloblastomas, treatment options include surgery, radiation, and chemotherapy. Unfortunately, complete surgical resection of the tumor bulk is not possible due to the infiltrative characteristics of the tumor that allow it to profusely invade surrounding tissue[36]. Tumor relapse is therefore inevitable in glioblastoma given that the remaining cells are able to repopulate the tumor. To address this issue, novel therapeutics are being investigated to specifically target and decrease the number of remaining CSCs within the tumor in order to delay relapse of the disease[37].

1.2 Daoy and U-87 MG Cell lines

For my studies, I used the Daoy and U-87 MG cell lines, which are representative of medulloblastoma and glioblastoma, respectively. Both cell lines were purchased from the American Type Culture Collection (ATCC) (Manassas, VA). The Daoy cell line was derived from a 4-year old Caucasian male patient with a medulloblastoma exhibiting desmoplastic nodular histology[38]. Therefore, this cell line has been extensively used in the study of the SHH medulloblastoma subtype.

The U-87 MG cell line was derived from a 44 year old female patient in 1968. Until recently, it was believed that the U-87 MG cell line available from ATCC was of this same origin. However, recent studies by Allen et al.[39] have shown that the U-87 MG cell line provided by ATCC is different from the cells expanded from the original tumor that was

excised in 1968. However, their studies conclude that the ATCC U-87 MG cell line was still likely derived from a human glioblastoma tumor.

A major difference between the two cell lines is that Daoy cells are p53 mutated, while U-87 MG cells are p53 wild-type. This is a relevant difference given that p53 mutations can alter the cellular response to DNA damage repair post-RT. In my studies, results showed different effects of TP508 on the Daoy and U-87 MG cell line. In Chapters 4 and 5 the role of p53 status and cellular response to radiation and TP508 treatment is further discussed.

Figure 1.4 show images taken in our laboratory of both Daoy and U-87 MG cells grown as attached 2D monolayers and as 3D spheres enriched for CSC survival. The Daoy cells form spheres with smooth borders, while the U-87 MG form spheres with amorphous borders, potentially indicating a more metastatic phenotype (Fig 1.4).

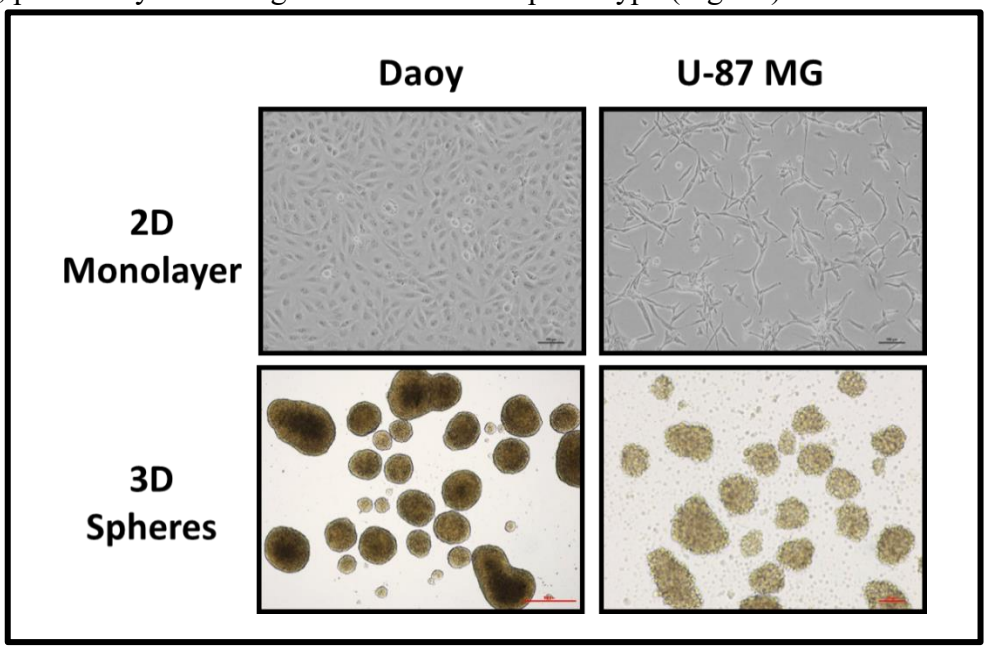

Figure 1.4: Medulloblastoma Daoy vs Glioblastoma U-87 MG Cells

1.3 Cancer Stem Cells

Cancer stem cells (CSCs) are a subpopulation of cancer cells within tumors with the ability to perpetually self-renew and differentiate, providing tumors with a limitless

supply of cancer cells[40-42]. They are believed to originate from normal stem cells transform into CSCs via mutations and genetic instability. As such, CSCs and normal stem cells share various characteristics, including the ability to self-renew and the common use of proliferative and pro-survival signaling pathways[43-45]. CSCs are also believed to derive from differentiated cancer cells that acquire stem-cell like characteristics via oncogene-induced plasticity[46]. Therefore, medulloblastoma appears to develop from normal stem cells that transform into cancerous cells via dysregulation of developmental pathways.

CSCs utilize pro-survival drug resistance mechanisms to evade cellular death. Some of these mechanisms include employing a more robust DNA damage repair system, adjusting their microenvironment to survive unfavorable conditions such as hypoxia, and dysregulating normal signaling pathways to increase proliferation[47]. To date, conventional treatment therapies are limited in their ability to circumvent these CSC survival mechanisms. Even if the tumor bulk shrinks in response to treatment and desirable outcomes are achieved, failure to eradicate these tumor-initiating CSCs results in the repopulation of tumors and relapse of the disease. Therefore, if CSCs can be specifically targeted and eradicated with treatment, then tumor recurrence can be eliminated[43, 48] (Fig 1.5). Given the importance of CSCs and their crucial role in relapse of disease, my goal was to determine whether TP508 exerted sensitizing effects on medulloblastoma CSCs. As such, in my studies, I examined the effects of TP508 (see section 1.8) on CSCs using established CSC markers, as described below.

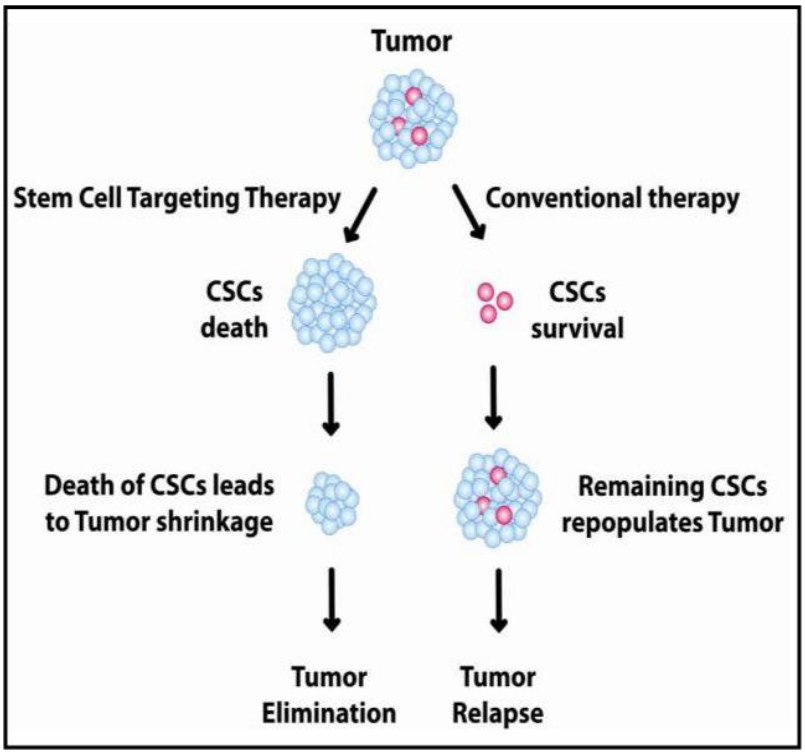

Figure 1.5: Cancer Stem Cell Hypothesis

Illustration by C. Kantara[1]

1.4 Cancer Stem Cell Markers

1.4.1 CD133

CD133 (prominin-1) is a pentatransmembrane glycoprotein that was found to be expressed at the surface of neural stem cells[49, 50]. In stage IV primary brain tumors, such as glioblastoma and medulloblastoma, high CD133 expression levels are associated with poor prognosis[51, 52]. In recent studies, *in vitro* tumorosphere assays were utilized to show that brain cancer cells expressing CD133 were able to proliferate, self-renew, and differentiate, while CD133-negative cells did not possess these cancer stem cell-like characteristics[53]. Furthermore, as few as 100 CD133-positive brain cancer cells were able to grow tumors in immunocompromised mice, while 100,000 CD133-negative cells failed to produce any

tumors[54]. These findings strongly suggested that CD133 is a marker of tumor-initiating brain cells, also known as CSCs.

1.4.2 CD44

CD44 is a cell-surface adhesion glycoprotein which mediates attachment to hyaluronic acid. It is involved in several processes including cell-cell interactions, cell migration and cell homing[55]. CD44 has been identified as a CSC marker in several tissues, including brain, colon and breast[56-59]. Tumors with an elevated expression of CD44-positive cells have been shown to possess enhanced metastatic and invasive abilities and are correlated with poor clinical prognosis[60]. Interestingly, studies have shown that targeting CD44 reduces tumor growth and relapse potential of xenografts in breast cancers[61].

1.4.3 LGR5

LGR5, also known as G-protein coupled receptor 49, is a Wnt target signaling gene[62] and has been established as a marker of cancer stem cells in various organs including brain, colon, prostate and pancreas[63-65]. LGR5 has also been found to be overexpressed in medulloblastoma and identified as a potential molecular target for medulloblastoma therapy[66].

1.5 Pluripotent Marker: Sox2

Sox2 is a transcription factor that has important regulatory roles in early pluripotent embryonic cells. Sox2 plays crucial roles in stem cell maintenance and reprogramming of somatic cells back towards pluripotency[67]. Various developmental issues have been associated with Sox2 mutations, given its primary role in stem cell development. Additionally, Sox2 dysregulation has been associated with several cancers, including the sonic hedgehog medulloblastoma subtype and glioblastomas[68, 69,70].

1.6 DNA Repair Mechanisms

For years, CSCs have been shown to have a unique ability to resist radiation exposure, minimize inflicted radiation-induced damage, and evade apoptosis[71] . The radio-resistant property of CSCs is believed to be due to their ability to activate a more rapid DNA repair response compared to normal stem cells, allowing them to escape cellular death[71]. Current brain cancer therapies, such as x-ray and gamma rays ionizing radiation, result in both single strand and double strand DNA breaks[72]. Single-strand breaks (SSBs) are well-tolerated by cells because the strand is able to ligate and repair itself rapidly. On the other hand, double-strand breaks (DSBs) are the most biologically lethal type of DNA damage and a major focus for developing novel radiotherapy cancer strategies[72]. Upon radiation-induced DSBs, a DNA damage response signaling cascade is activated and triggers a chain of events which include: 1) identification of the damage, 2) arrest of the cell cycle and 3) DNA repair via NHEJ (non-homologous end joining) or HR (homologous recombination)[73, 74] (Fig 1.6). In some cases, cells are damaged to an irreparable extent and are thus prohibited from exiting the cell cycle arrest[73]. Instead, they either undergo apoptosis or initiate cell senescence[73, 75]. However, in the event cells can be repaired, selection and activation of the appropriate repair pathway is dependent on the phase at which the cells were cycling through at the time of the damage. For instance, the high fidelity HR repair pathway is activated during the late S and G2 phases of the cell cycle as it requires an undamaged sister chromatid as a template to repair the cell[76] (Fig 1.6). In contrast, the NHEJ repair pathway becomes activated throughout the entire cell cycle[76] (Fig 1.6). This pathway is more prone to errors and repairs the cells by directly ligating the broken DNA ends which allows for deletions and insertions to occur[73, 74]. There is a Classical-NHEJ and an alternative-NHEJ process that can take place upon DNA damage. The Classical-NHEJ is the primary pathway for DSB repair, while the alternative-NHEJ is activated when there is a dysregulation of normal repair processes[77]. As such, alternative-

NHEJ is more error-prone; it also utilizes distinct set of proteins that are important in the repair of single-stranded breaks. Therefore, for the purpose of my studies I focused on the key molecules involved in the Classical-NHEJ, given that they are the predominant repair proteins activated upon DSBs.

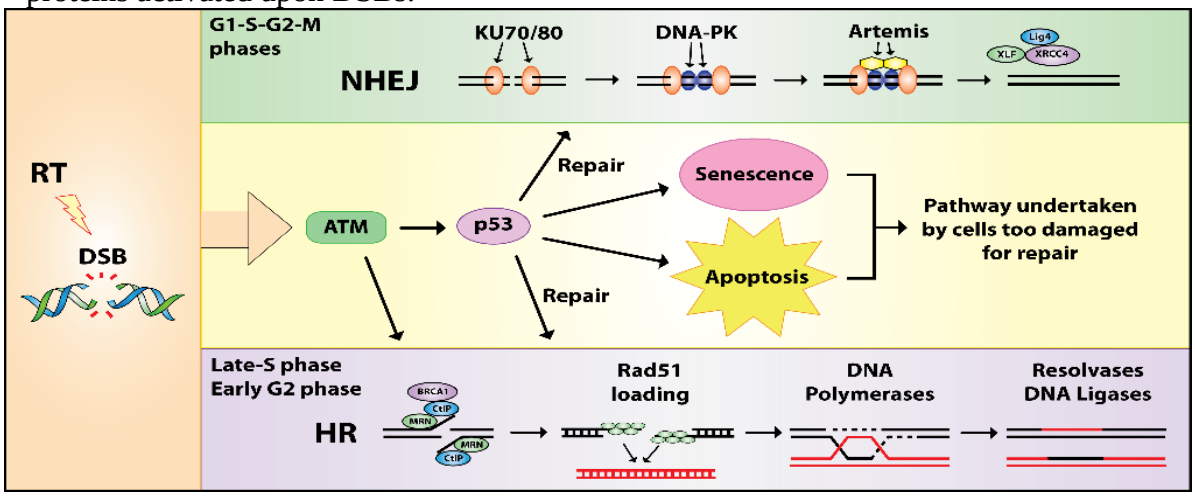

Figure 1.6: Activation of DNA DSB Repair Pathways Post-Radiation Exposure

Both HR and NHEJ repair pathways are mediated by sensors, mediators and effectors which are essential in correcting the DNA damage. Ku70 and Ku 80 (sensors), DNA-PK (transducer) and DNA ligase IV, XRCC4 & XLF (effectors) are all part of the core components of NHEJ repair pathway (Fig 1.6). On the other hand, the MRN (Mre11-Rad50-NBS1) complex, BRCA1 & CtIP (sensors), ATM (transducer) and RAD51 (effector) are the core components of the HR repair pathway (Fig 1.6). The sensors are responsible for identifying the DNA damage and activating corresponding transducers[73]. Subsequently, these transduction kinases in turn phosphorylate checkpoint kinases to induce cell cycle arrest and activate the required effectors for repair.[78] Current studies focus on developing novel therapeutics capable of inhibiting/down-regulating repair sensors, mediators, and effectors in order to halt DNA repair mechanisms of CSCs and promote cell death. Therefore, in my studies I examined the effects of TP508 on DNA DSBs and repair mechanisms involved in medulloblastoma CSCs. The goal was to examine whether TP508 may promote DNA damage by targeting HR or NHEJ molecules and thereby

preventing/delaying repair of CSCs post-RT. If successful, the drug could potentially be used in combination with radio/chemotherapy to help sensitize CSCs to RT.

1.7 Radiosensitizers

To date there are no FDA approved radiosensitizers available to treat cancers, including medulloblastoma[79, 80]. In clinical trials, radiosensitizers are being administered prior to treatment in order to render cancer cells more susceptible to RT, thereby increasing the effectiveness of radiation[79]. However, current radiosensitizers in clinical trials are only focused at targeting the tumor bulk and not the tumor-initiating CSCs[81]. Recently, conventional chemotherapy drugs such as 5-Fluorouracil and Gemcitabine have been tested in clinical trials as potential radiosensitizers for cervix, esophagus, and pancreatic cancer[81]. A non-exhaustive list of potential radiosensitizers and their mode of action is listed in Table 1.1. However, these drugs exert numerous side effects on patients, lack the ability to target CSCs, and are currently not being tested in medulloblastomas[81].

Radiosensitizers	Method of Action
Hyperbaric oxygen	Increases the oxygen tension, producing more free radicals, in radioresistant hypoxic tumors
Nucleoside analogs (5-FUra, BrdUrd, IdUrd)	Incorporation into DNA to prevent radiation-induced DNA damage repair
Taxanes	Promote accumulation of cells at G2/mitosis phase (most radiosensitive phase)
Irinotecan	Targets topoisomerase I, leading to cell death
Hyperthermia	Elevates temperature to increase membrane fluidity and inhibit macromolecular synthesis
Sulfhydryl group suppressors	Depletion of sulfhydryl groups (known radiation damage protectors)
Checkpoint kinase inhibitors	Promote cell cycle progression with damaged DNA, leading to cell death

Table 1.1: Potential radiosensitizers and their respective mode of action. Adapted from Raviraj et al.[79]

1.8 Thrombin Peptide TP508

Thrombin peptide TP508, also known as rusalatide acetate or Chrysalin®, is a 23-amino acid synthetic peptide representing a portion of the human prothrombin with a sequence of AGYKPDEGKRGDACEGDSGGPFV (Figs 1.7 and 1.8). TP508 corresponds to amino acids 508-530 of the prothrombin or 183-200 of the α-thrombin peptide. Thrombin plays an important role in the coagulation cascade by converting soluble fibrinogen into the insoluble fibrin required for blood clot formation[82]. Upon vascular injury, prothrombin is proteolytically cleaved by activated factor X, yielding the biologically active α-thrombin[82] (Fig 1.7). The biological activity of the TP508 sequence was discovered by screening molecules that could bind to high-affinity thrombin receptors and mimic cellular effects of thrombin at sites of tissue injury[83, 84]. Thus, TP508 was selected for its interaction with a subset of high affinity non-proteolytic activated receptors (NPARs). Early studies demonstrated specificity of TP508 binding and crosslinking to the NPAR receptor, specific signaling cascades that included activation of endothelial nitric oxide synthase, PI3K, SRC, AKT and PKC[85]. Although a great deal has been published on the activity of this peptide, the specific receptor for TP508 has not yet been identified, and thus the TP508-NPAR interaction and how it relates to current studies is yet to be fully elucidated.

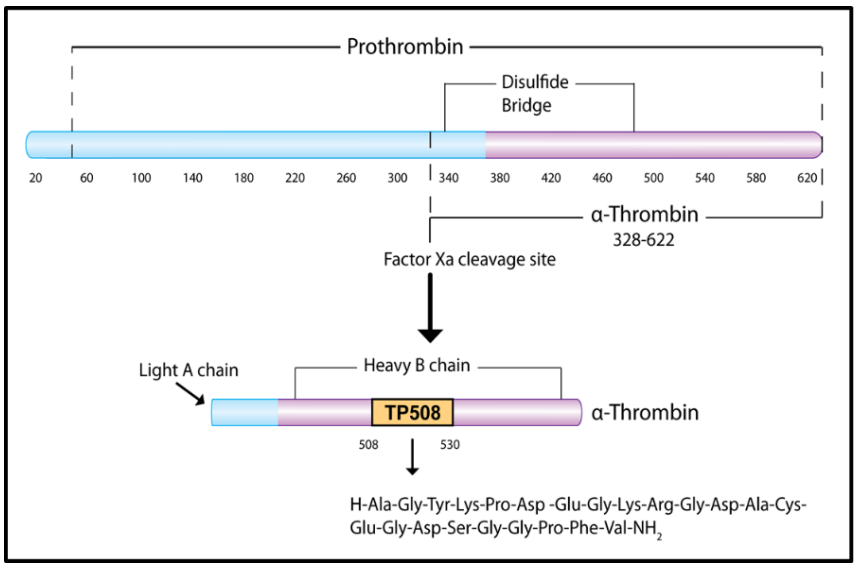

Figure 1.7: TP508 Structure: Cleavage of prothrombin into α-thrombin

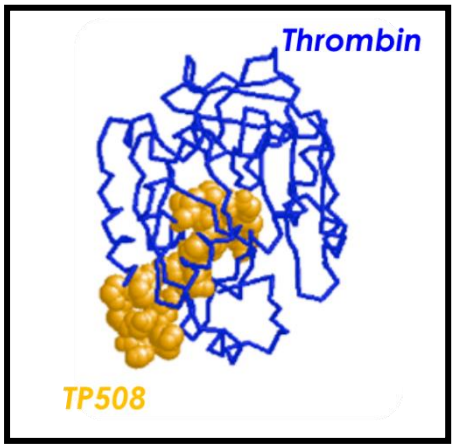

Figure 1.8: TP508 Structure

Blue: Thrombin
Gold: TP508

TP508 was developed as a wound and fracture repair drug[86]. It has been shown to stimulate angiogenesis[87, 88], reverse endothelial dysfunction[89], accelerate closure in dermal wounds in various animal models[90, 91], accelerate bone fraction repair[92], and stimulate bone formation during osteogenesis[93]. TP508 has been tested in clinical trials to treat diabetic foot ulcers (phase I/II)[94] and bone fractures (phase II/III)[95] in over 600 patients without any drug related adverse events.

More recently, TP508 has shown promising potential as a nuclear countermeasure drug. Systemic delivery of TP508 24-hours post-total body irradiation has been shown to increase survival in mice by activating stem cells within intestinal crypts and thereby mitigating the effects of radiation-induced gastrointestinal toxicity[96]. Additionally, the peptide has been shown to accelerate DNA damage repair in human dermal vascular endothelial cells and restore endothelial function post-radiation damage[97].

A brief overview of TP508 findings in various studies is illustrated below (Fig 1.9).

Figure 1.9: TP508 Applications

1.9 Preliminary Studies

In preliminary studies, conducted in collaboration with Dr. M. Waleed Gaber's laboratory at Baylor College of Medicine, TP508 was shown to exert regenerative and protective properties on neuronal cells post-radiation exposure. In these studies, 8-week old mice were treated with either saline or TP508 intravenously 1 hour before a 7Gy dose of radiation to the hippocampal region of the brain. The mice were then imaged using

diffusion tensor imaging, a magnetic resonance imaging technique that estimates white matter connectivity patterns in the brain[98]. Results showed that mice treated with saline and exposed to radiation had a substantial decrease in neuronal integrity post-RT as compared to the non-irradiated group. However, the neuronal integrity of mice treated with TP508 1 hour before radiation was protected, as evidenced by white matter connectivity patterns that were similar to the non-irradiated group.

In addition, preliminary studies were conducted to examine whether the protection of neuronal integrity could be due to TP508 protecting or stimulating stem cells in the hippocampus. Immunofluorescent staining of mouse brains collected 3 months post-RT showed a substantial increase in the expression of stem cell marker, Nestin, and proliferative marker, PCNA, in the TP508 treated group as compared to the control irradiated brains. These results suggested that TP508 may stimulate proliferation and activate neural stem cells in the hippocampus post-radiation injury.

In vitro studies were then conducted with normal neural stem cells treated with saline or TP508 1hour prior to receiving a 2Gy dose of radiation. The cells were then analyzed using immunofluorescent staining probing for stem cell and proliferative markers. The findings showed that non-irradiated normal neural stem cells express high levels of proliferation and of stem cell markers, Nestin, LGR5 and pluripotent marker Sox2. Within 24 hours of being exposed to radiation, the expression levels of Nestin, LGR5, Sox2 were depleted and the cells were no longer proliferating. However, when treated with RT and TP508, the expression levels of the stem cell markers were rescued and the cells were actively proliferating. This data suggested that TP508 was protecting the neural stem cells from RT-induced damage.

Overall, the data thus far suggested that TP508 was exerting protective effects on normal neural stem/progenitor cells and promoting neurogenesis[99]. Therefore, it was imperative to determine whether TP508 would also protect cancer cells from radiation and/or interfere with radiation-induced tumor shrinkage. To address this concern, tumor-

bearing mice were injected with TP508 24h before radiation therapy and were monitored for tumor growth via magnetic resonance imaging. Interestingly, results showed that TP508 *increased* RT-induced tumor shrinkage post-treatment (Fig 1.10). Note the reduction in tumor size post-treatment in the TP508 treated tumor (bottom image) vs control tumor (top image). The tumors have been highlighted in yellow for ease of visualization. These results suggested that not only did TP508 *not* interfere with tumor shrinkage, it essentially promoted brain tumor shrinkage in mice. This experiment suggested that TP508 was behaving as a radiosensitizer by making the tumor more susceptible to radiation damage. Therefore, I developed my dissertation project with the goal to explore the potential role of TP508 as a radiosensitizer of brain cancer cells. Results of my studies are discussed in Chapter 3 and 4.

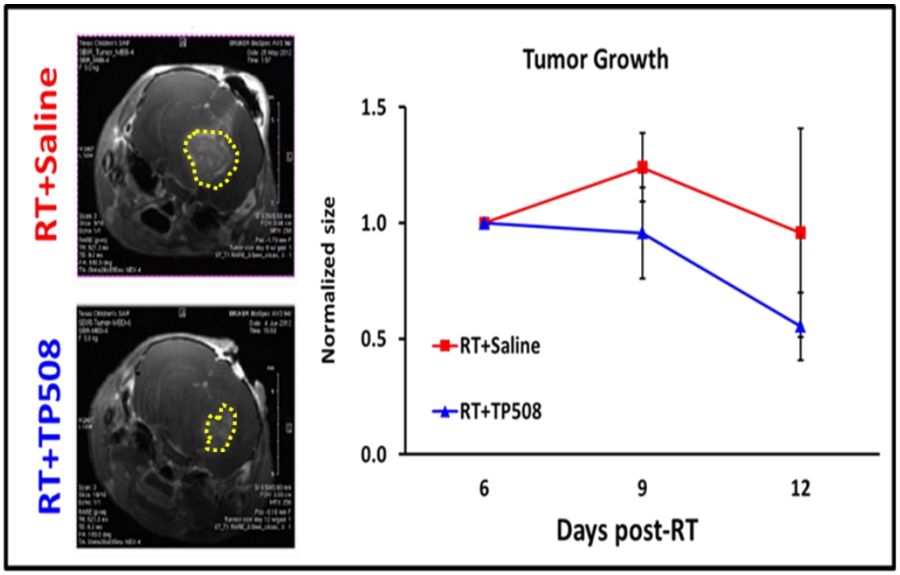

Figure 1.10.: Magnetic resonance images showing glioblastoma tumor shrinking effects of TP508.

Mice were implanted with glioblastoma U-87 MG cancer cells and tumors were allowed to grow. Four weeks later, mice were treated with Saline or TP508 (12.5mg/kg) intravenously 1hour before receiving a 7Gy radiation dose. Mice were imaged at Day 12 post-RT. Tumors are highlighted in yellow for visualization. Studies were conducted by M. Waleed Gaber laboratory at Baylor College of Medicine.

CHAPTER 2: MATERIALS AND METHODS

2.1 Materials

Thrombin peptide TP508 (AGYKPDEGKRGDACEGDSGGPFV, rusalatide acetate, CAS no. 87455-82-6) was synthesized and purified by American Peptide Company (now Bachem Americas Inc., Sunnyvale, CA) and supplied as a lyophilized powder. Sterile 0.9 percent saline for reconstitution of TP508 and for animal injections was purchased from Hospira (Lake Forest, IL). Antibodies used in this study include: anti-CD44 (#3578S), anti-Sox2 (#4900s), anti-phospho-Chk1 (Ser 345) (#2348), anti-phospho-Chk2 (Thr 68) (#2197), anti-p-BRCA1 (Ser 1524) (#9009), and anti-Rad50 (#3427) (Cell Signaling Technology, Danvers, MA); anti-proliferating cell nuclear antigen (PCNA) (ab29), anti-GPCR GPR49 (Lgr5) (ab75850), anti-active caspase-3 (ab13847) (Abcam, Cambridge, MA); β-actin (A3854) (Sigma-Aldrich, St. Louis, MO); and anti-CD133 (PA5-38014) (ThermoFisher Scientific, Waltham, MA). Alexa Fluor-488 and Alexa-Fluor-594 coupled-secondary IgG antibodies and 4',6-diamidino-2-phenylindole (DAPI) were purchased from ThermoFisher Scientific (Waltham, MA).

2.2 Preparation of Lyophilized TP508

As stated above, TP508 is synthesized by American Peptide company as a lyophilized powder and diluted with 0.9 percent saline. The volume of saline necessary to dilute the peptide depends on the desired stock concentration, the percent peptide content, and percent peptide purity of the specific lot number. The TP508 was reconstituted in sterile conditions and was aliquoted and stored at -80° C in low-protein binding tubes. Final protein concentration was tested by using the BioTek microplate spectrophotometer and Take3 microplate protein quantification system (BioTek Instruments, Inc., Winooski, VT).

2.3 Cell culture

Daoy cells (HTB-186) and U-87 MG (HTB-14) cells were purchased from the American Type Culture Collection (Manassas, VA) and cultured in minimum essential medium (EMEM) supplemented with 10 percent fetal calf serum and 1 percent penicillin/streptomycin. The cells were maintained in a 37°C incubator with 5 percent CO_2. The cell lines were authenticated by BioSynthesis DNA Identity Center in 2013.

2.4 Spheroidal Assay

Daoy cells were grown as 3D spheres *in vitro*, as described by Kantara et. al[100] (Fig 2.1). Monolayer cells were re-suspended and plated at a density of 30000 cells/well into 24-well ultra-low-attachment plates (Costar, Corning N.Y.), in 500µL serum-free DMEM/F12(1:1) media containing 1 percent Antibiotic-Antimycotic (100×) supplemented with B-27 (50×) (Invitrogen), epidermal growth factor (EGF) 20 ng/ml and fibroblast growth factor (bFGF) (10 ng/ml) (Sigma-Aldrich, St Louis, Mo.). Media was changed every 2-3 days by tilting the plate, allowing the spheres to pool towards the bottom edge of the plate, and aspirating half of the total media volume and replenishing with fresh media. Formation of spheres was monitored once daily. Spheres were imaged with an

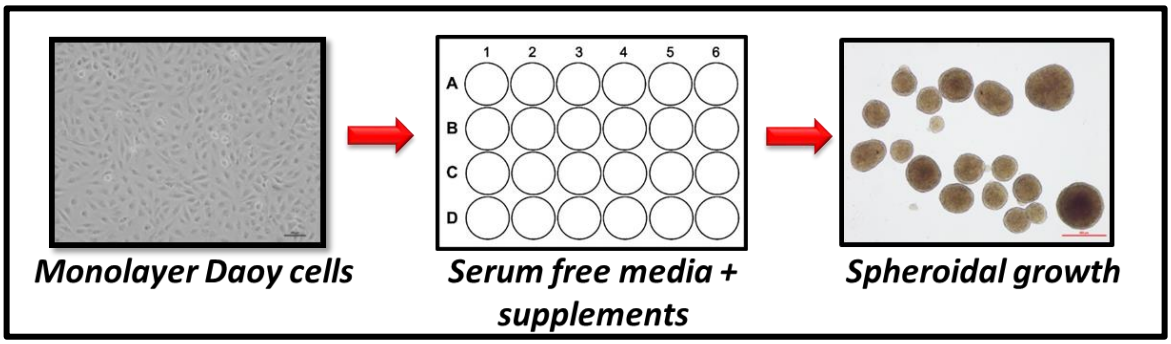

Figure 2.1: Spheroidal Assay

inverted microscope, at 4x, 10x and 40x using white light microscopy (Nikon Eclipse TS100, Melville, N.Y.).

In preliminary experiments, cells were plated at increasing numbers to optimize the spheroid assay. Based on the results, an optimal number of 30000 cells were chosen for growing primary spheres from Daoy medulloblastoma and U-87 MG glioblastoma cells.

2.5 Irradiation of cells

Neurospheres were irradiated at a dose rate of 4.37 Gy/min using a cesium source irradiator. The Mark 1 irradiator 137Cs, was operated by Dr. Bradford Loucas in Brackenridge Hall at UTMB. Neurospheres were plated in 24-well plates and two plates were irradiated at the same time by placing them in the center of the irradiator's rotating chamber. In order to confirm radiation dose, Landauer® nanoDot™ OSLD dosimeters were placed on the exterior of the plates and sent to the manufacturer (Landauer, Glenwood, IL) for analysis.

A diagrammatical representation of treatment and irradiation of neurospheres is depicted in Figure 2.2. Cells were plated for spheroidal formation and allowed to grow for 5 days. At day 5, fully formed primary neurospheres were treated with either saline or TP508 (0.5 mg/mL). On day 7, neurospheres were exposed to a 10Gy dose of radiation (Daoy) or 30Gy dose (U-87 MG). Different treatment and radiation doses were tested in preliminary studies (Fig 2.3). Results showed that when spheres were treated 48 hours pre-radiation therapy there was a more robust decrease in the formation of secondary spheres as compared to treating them 24 hours pre-radiation therapy (Fig 2.3Ai-ii). Additionally, both 20Gy and 30Gy doses were effective in reducing the number of secondary spheres, with the most significant differences observed at 0.33 and 1mg/mL TP508 concentrations (2.3Bi-ii). A final radiation dose of 10Gy and 0.5mg/mL TP508 dose 48 hours pre-RT was then tested and chosen as the treatment combination for optimal results (data presented in

this body of work). Specific collection and analysis protocols of neurospheres post-radiation was then determined based on each experimental endpoint.

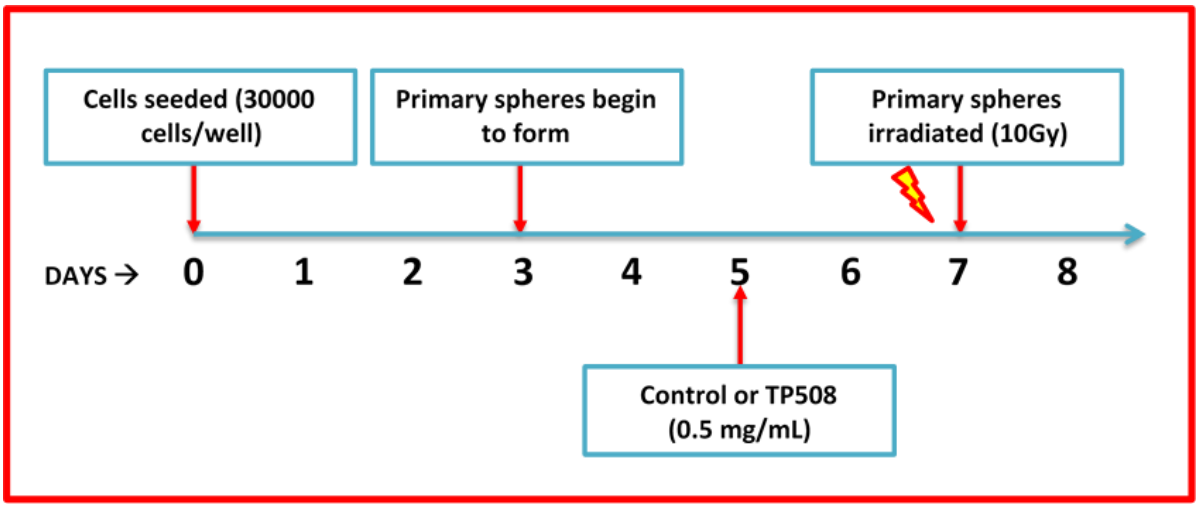

Figure 2.2: Timeline of Irradiation of Spheres

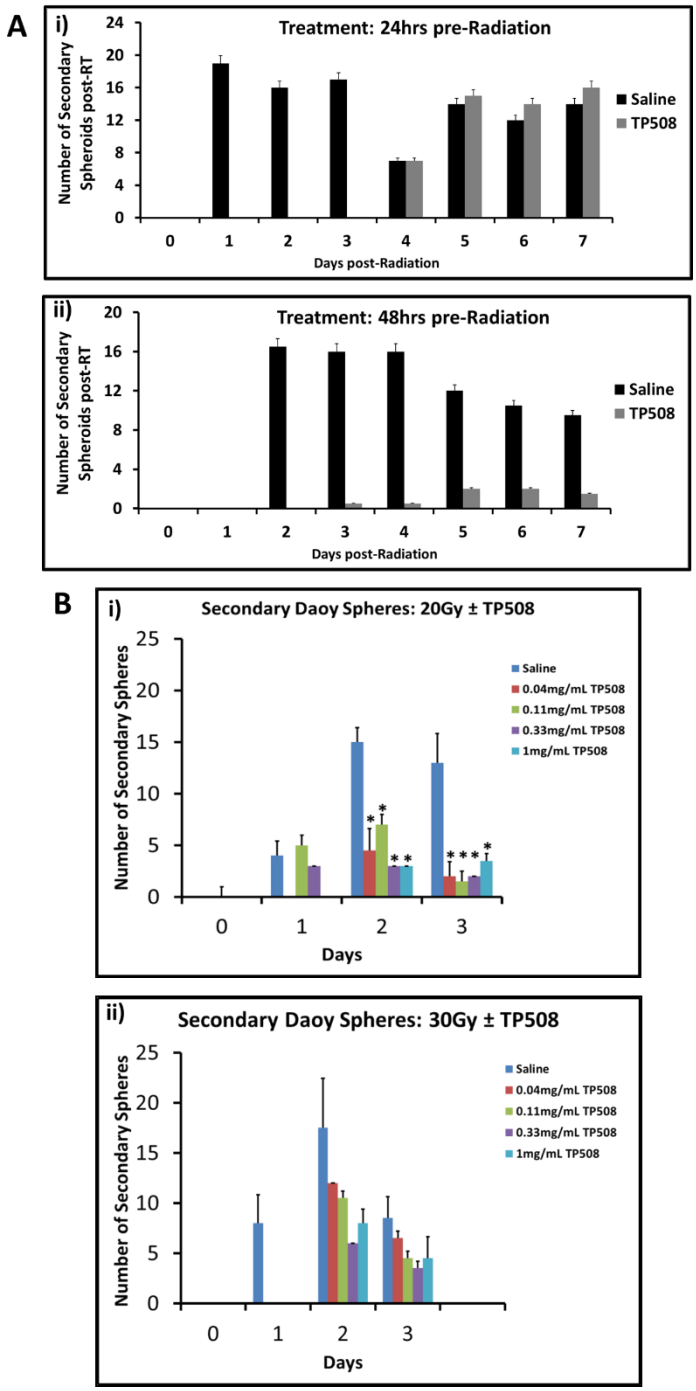

Figure 2.3 Optimization of treatment timing, TP508 dose, and radiation dose

Ai-ii) Number of secondary Daoy spheres formed post-radiation therapy when spheres were treated 24 and 48 hours pre-RT. Data are presented as mean ± standard deviation of two wells/three experiments. Bi-ii) Number of secondary Daoy spheres formed post-radiation therapy when spheres were exposed to 20Gy and 30Gy radiation doses and treated with either saline or ranging doses of TP508 (0.04, 0.11, 0.33, and 1 mg/mL). Data are presented as mean ± standard deviation of two wells/three experiments. *=P<0.05 vs control values.

2.6 Secondary Sphere Formation

For generating secondary spheres, cells were grown as spheres, as previously described, and were then enzymatically dissociated with Trypsin 0.25 percent into single cells immediately after radiation exposure (10Gy for Daoy and 30Gy for U-87 MG). The dissociated single cells were then re-plated in low-attachment plates as secondary spheres (Fig 2.4). Their re-growth and formation was monitored daily and images were taken daily using white light microscopy (Nikon Eclipse TS100, Melville, N.Y.)

2.6.1 Cell viability of spheres post-radiation therapy

The cell viability of spheres was analyzed daily by mechanically dissociating the spheres into single cells and using the Trypan blue dye exclusion assay and the Cellometer mini counter (Nexcelom Bioscience, Lawrence, MA).

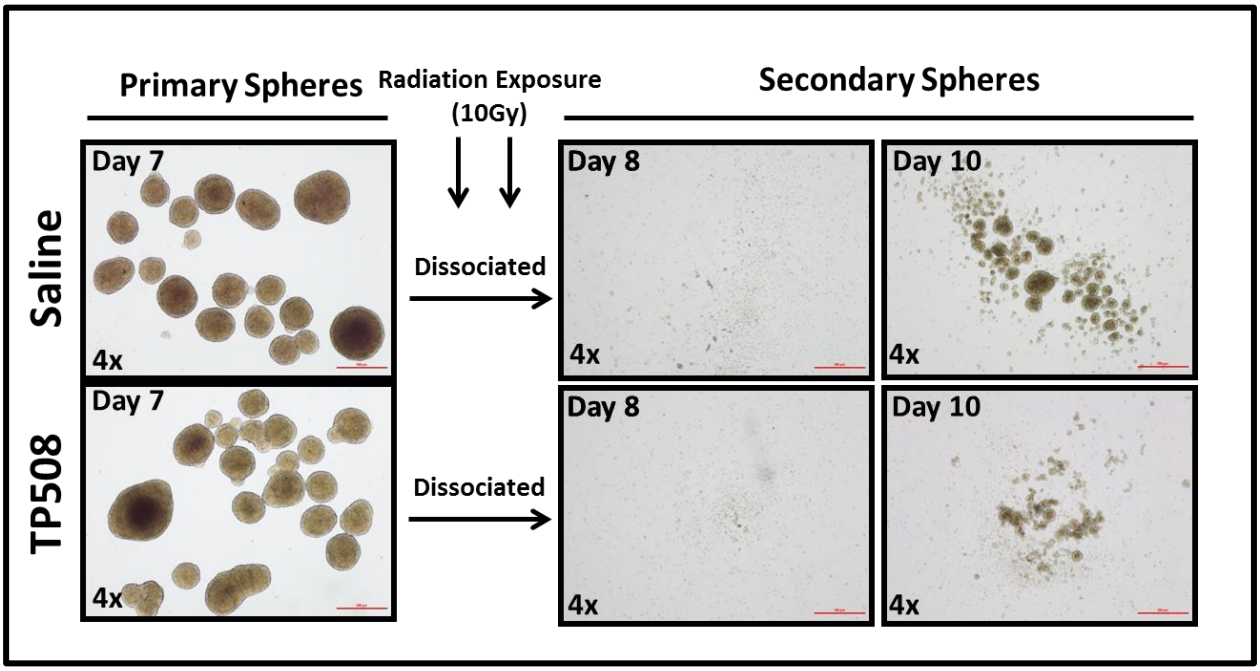

Figure 2.4: Secondary Sphere Formation Assay of Daoy neurospheres

2.7 Immunoblot Analysis

Neurospheres were lysed and underwent sonication in RIPA (radioimmunoprecipitation assay) buffer supplemented with protease cocktail inhibitor. After sonication, lysed cells were centrifuged at 4°C at 8000rpm for 5 minutes, and the supernatant was stored at -80° for immunoblotting.

The protein concentration of each lysate was determined using the BCA (Bicinchoninic acid) assay (ThermoScientific, Waltham, MA) and BioTek Synergy Hybrid plate reader. Approximately 10-20 micrograms of total proteins per treatment group were loaded onto a 10 percent polyacrylamide gel, separated by electrophoresis, and transferred to a PVDF (polyvinylidene fluoride) membrane, as described by Kantara et al[96]. Blots were cut horizontally into strips based on the molecular size of the target or loading control protein. All antibodies were diluted in 5 percent milk in TBST (tris-buffered saline (TBS) and Tween 20) at a dilution of 1:100-500, except for β-actin that was diluted at 1:30000 and PCNA that was diluted at 1:5000. Blots were incubated overnight at 4°C and washed 3 times with TBST before incubation with secondary antibodies (dilution 1:5000) for 1 hour at room temperature in 5 percent milk in TBSTrea . Blots were then washed 3 times with TBST before antigen-antibody complexes were detected using a chemiluminescent reagent kit (GE Healthcare, Piscataway, NJ).

Immunoblot data was quantified using the NIH Image J software (National Institutes of Health, Bethesda, MD) by calculating the density of the bands as a percent ratio change of target protein/β-actin (loading control).

2.8 Immunofluorescent Staining

Cell/tissue sections were deparaffinized, rehydrated, and boiled in antigen retrieval for 5 minutes before staining with target antibodies. Tissues were blocked with 5 percent goat serum diluted in immunofluorescent blocking solution (1% BSA in PBS). Antibodies

were all diluted at 1:100, incubated overnight at 4°C, washed 3 times with blocking solution and incubated at room temperature with secondary fluorophore-conjugated antibodies for 1 hour. Slides were washed with PBS 3 times and incubated with DAPI (blue nuclear staining) for three minutes before coverslipping and using a Fluorsave reagent (EMD Millipore, Darmstadt, Germany). Images were then taken using an epifluorescent microscope (Zeiss Axioplan) and Metamorph Software. Staining was analyzed using Image J software by calculating the percent area staining of the target protein per the percent area staining of nuclei staining (DAPI). Cells/tissues were collected as follows:

2.8.1 Neurospheres

Neurospheres were fixed in 10 percent formalin for 12 hours and then transferred to a microtube containing 2 percent agar gel with 0.05 percent sodium azide. Tubes were stored at -20°C for 5 minutes in an inverted position to solidify the gel and were then left inverted overnight at 4°C. The next day, the cone-shaped agar containing the intact spheres were processed for paraffin embedding. The paraffin blocks were cut into 4µm sections onto microscope slides for immunofluorescent (IF) and hematoxylin and eosin (H&E) staining.

2.8.2 Xenograft tumors

Tumors were excised from athymic nude mice and immediately submerged in 10 percent formalin. After 24 hours, tumors were transferred to a 70 percent ethanol solution and processed for paraffin embedding. The paraffin blocks were cut into 5µm sections onto microscope slides for IF and H&E staining.

2.9 Flow Cytometry

Spheres were grown as described above, treated on day 5, irradiated on day 7, and collected for flow analysis 3 days post-RT. Spheres were collected in microtubes, washed with PBS, and trypsinized with 0.25 percent Trypsin into single cell suspension. Single cells were strained through a 35mm nylon mesh and brought to 1mL volume.

Antibody-conjugated fluorophores were added to the cells (dilution 1:100) in their respective microtubes. The tubes were covered in foil to protect the fluorophores from the light, and were left at room temperature for 1 hour.

Cells were washed 3x at 1200rpm with flow cytometry buffer (1% BSA in PBS) and resuspended in a final volume of 500μL of the flow cytometry buffer. Cells were analyzed using the BD LSRII Fortessa flow cytometer.

2.10 Animal experiments

All experiments were conducted at the University of Texas Medical Branch (UTMB) following an IACUC-approved protocol. Athymic 5-6 week old mice (Taconic, Hudson, NY) were housed 3 per cage and allowed to acclimate for at least seven days in the Animal Research Center at UTMB before initiation of experiments.

Preparation of cells: On the day of injection neurospheres were collected in a 1.5 mL sterile microtube and centrifuged at 1000 rpm for 5min. Supernatant was discarded and neurospheres were washed 3 times with sterile saline. Neurospheres were dissociated and analyzed for cell viability. Cells with viability results below 60 percent were not used for injection. Cells were then resuspended to desired final concentration in a 1.5mL sterile tube and kept on ice at all times until injection.

Inoculation of pre-treated and pre-irradiated tumor cells: Daoy neurospheres were treated plus or minus TP508 and exposed to radiation before being injected into mice. The

mice were anesthetized using isoflurane and 3-5x10^6 Daoy cells were injected subcutaneously bilaterally in the flanks using a tuberculin syringe at a volume of 100 µL per flank. Tumors were measured with a caliper three times per week. Tumors were allowed to grow until they reached the maximum allowed size (2000mm^3). (Fig 2.5)

Inoculation of tumor cells: The mice were anesthetized using isoflurane and 3-5x10^6 Daoy cells were injected subcutaneously bilaterally in the flanks using a tuberculin syringe at a volume of 100 µL per flank. Tumors were measured with a caliper three times per week. Tumors were allowed to grow until they were approximately 200mm^3 before irradiation. (Fig 2.6)

Treatment and irradiation of tumors: Mice were injected with either 0.9 percent saline (150µL) or TP508 (25 mg/kg) subcutaneously, 1 hour prior to radiation (6Gy). After 23 hours the mice were injected again with saline or TP508 (25mg/kg) and were irradiated 1 hour later (6Gy). Thus, the total dose of TP508 was 50mg/kg and the total dose of irradiation was 12Gy. Lead shielding was used to protect the mouse and expose only the tumors to the x-ray source (RS2000, Radsource, 160kVp, 25 mA, 2.677 Gy/min). In order to confirm radiation dose, the RS2000 Accugold dosimeter probe was used prior to each experiment.

2.11 Statistical Analysis

Data are presented as a mean ± standard deviation of a minimum of three experiments. The Student-T test was used to determine p-value by comparing the treatment group to the control. P-value significance was set at < 0.05.

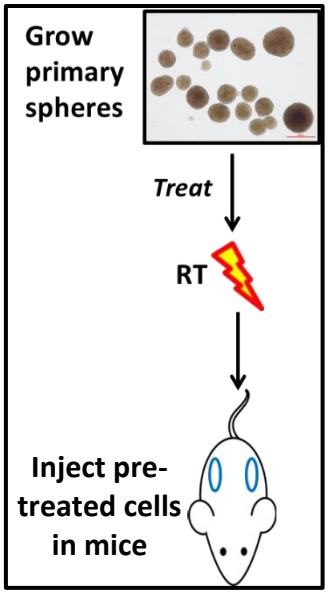

Figure 2.5 Experimental design of *in vivo* tumor growth of pre-treated cells

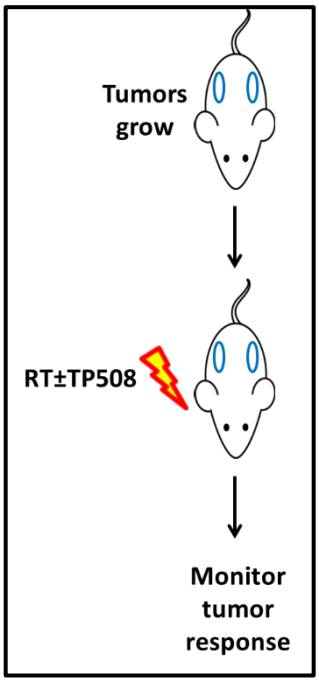

Figure 2.6: Experimental design of *in vivo* tumor growth after systemic TP508 injection

CHAPTER 3: TP508 RADIOSENSITIZES CANCER STEM CELLS AND DELAYS TUMOR RELAPSE

Introduction

As previously discussed, results from previous studies showed that TP508 protected normal neuroprogenitor cells from radiation-induced damage by protecting the expression of neural stem cell (Nestin, LGR5), pluripotent (Sox2), and proliferative (PCNA) markers (Fig 1.11). A major concern with drugs that may protect normal cells from damaging effects of radiation therapy (RT) is whether they may also protect cancer cells. Therefore, in these *in vitro* and *in vivo* studies I sought to determine whether TP508 could potentially protect cancer stem cells (CSCs) from radiation treatment. For these experiments, I used cells from different stage IV primary brain tumor types. Daoy medulloblastoma cells and U-87 MG glioblastoma were grown as neurospheres using a 3D-culture spheroidal assay which selects for the survival and growth of stem cells[100-102]. The ability for CSCs to form secondary neurospheres post-RT is an indicator of the stemness potential of these cells. Therefore, neurospheres were treated with either saline or TP508, exposed to radiation 48 hours later, and dissociated 24 hours thereafter to allow for the formation of secondary spheres.

Results

TP508 decreases cell viability, tumor heterogeneity and relapse potential of medulloblastoma cancer stem cells in vitro, post-RT

Daoy neurospheres were grown and treated plus or minus TP508 (0.5mg/mL) and exposed to 10Gy of radiation 48h post-treatment. Optimal drug dosing, treatment time, and radiation exposure were determined prior to the start of these experiments (Fig 2.2). Neurospheres were dissociated into single cells immediately after radiation, re-seeded, and

allowed to re-form as secondary neurospheres. Images were taken daily to assess the ability for the cells to form neurospheres given that the rate of formation of secondary spheres is an indicator of stemness potential (Fig 3.1 Bi). Viability of secondary neurospheres was also examined daily using Trypan blue dye exclusion testing to determine effects of TP508 on CSC viability post-RT. Interestingly, results showed that the cell viability of TP508 treated neurospheres was significantly ($p<0.05$) decreased at days 3-4 post-RT, as compared to the saline control treated neurospheres (Fig 3.1A),. Additionally, the rate of formation of secondary neurospheres was delayed in the TP508 treated group (Fig 3.1Bi-ii) as compared to the control. While secondary neurospheres began to form at day 2 post-RT in the saline group, secondary spheres did not begin to form until day 4 post-RT in the TP508 treated group. The size of the neurospheres were measured using a pre-set scale available in the imaging *NIS Element* software. Larger neurospheres characterize a more heterogeneous population of CSCs, whereas smaller neurospheres represent a less heterogeneous CSC population. Increased heterogeneity is associated with a more resistant CSC population in tumors, which in turn requires more robust and aggressive radio/chemo treatment regimens[103]. Results show that the size (μm) of the secondary neurospheres was significantly smaller ($p<0.05$) in the TP508 treated group, at days 2 and 3 post-RT (Fig 3.1Biii).

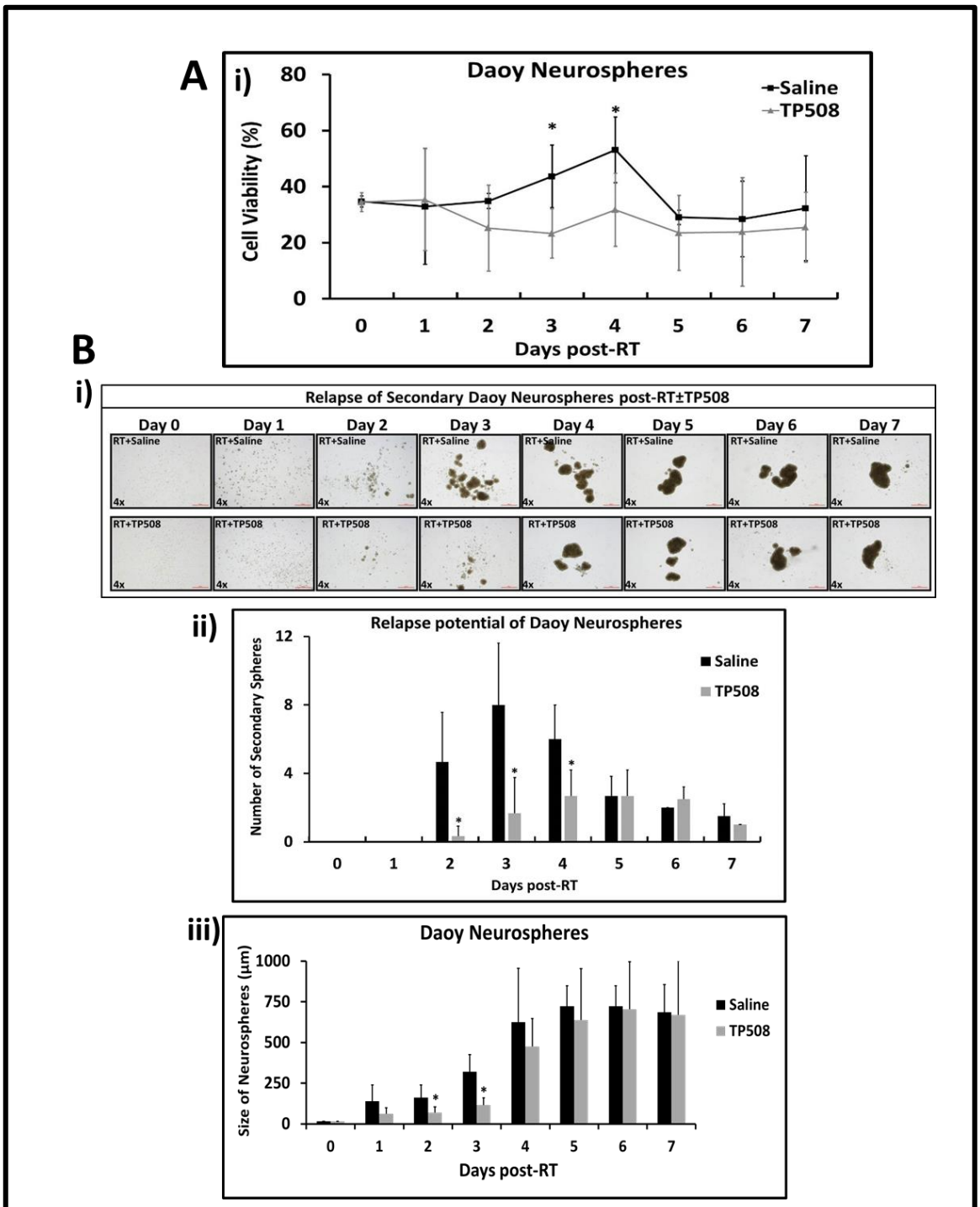

Figure 3.1 Effects of TP508 on spheroidal viability and stemness post-RT

A) Cell viability (percent) of Daoy neurospheres post-RT. Data are presented as mean ± standard deviation of six wells/day/five experiments. *=P<0.05 vs control values. B) i) Representative images taken at 4x of Daoy neurospheres dissociated post-RT and re-seeded for secondary neurosphere formation. ii) Bar graph illustrating the number of secondary neurospheres formed post-RT. iii) Bar graph illustrating the size of secondary neurospheres (µm) post-RT. Data are presented as mean±standard deviation of six wells/day/five experiments. *=P<0.05 vs control values.

TP508 decreases medulloblastoma cancer stem cell proliferation and expression of stem cell markers, while increasing apoptosis.

Daoy neurospheres were treated and irradiated as described above and collected at day 4 post-RT for Western blot analysis. Day 4 post-RT was chosen given that the difference in viability (Fig 3.1A) between the saline control and TP508 group was largest at this time point. The neurospheres were lysed and sonicated in RIPA buffer and the protein concentration was determined using the BCA protein assay. Cell lysates were probed for cancer stem cell markers, CD133, LGR5, CD44 and pluripotent marker, Sox2. Results showed that the expression of these markers was significantly decreased in the 10Gy+TP508 group as compared to the 10Gy+Saline group ($p<0.05$) (Fig 3.2A-B). Additionally, the expressions of proliferative marker PCNA is decreased, while the apoptotic marker, activated caspase-3, is increased in the TP508 vs saline group (Fig 3.2A-B).

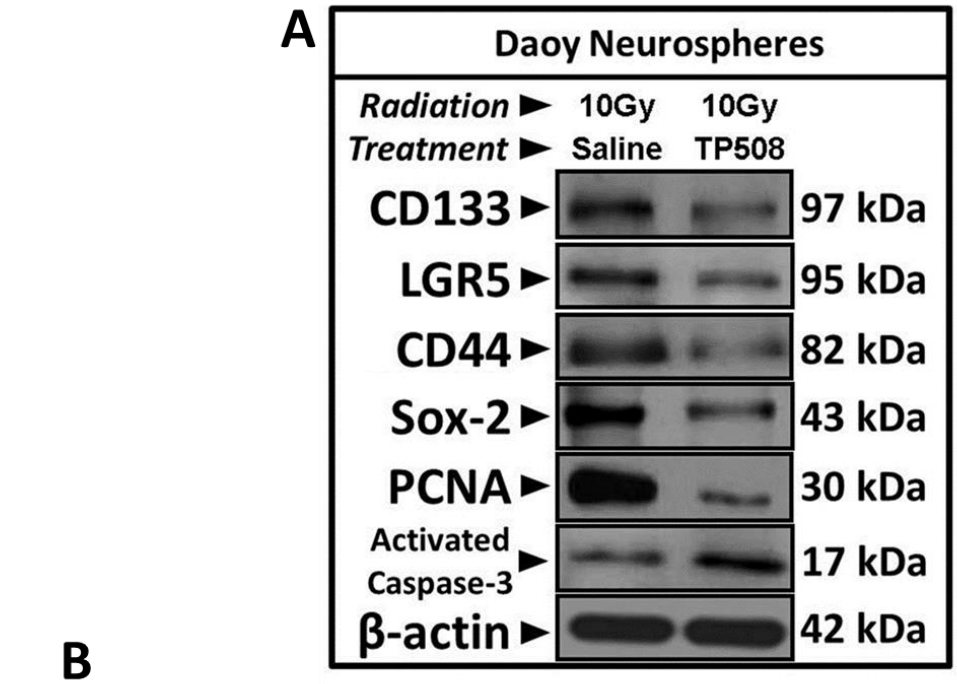

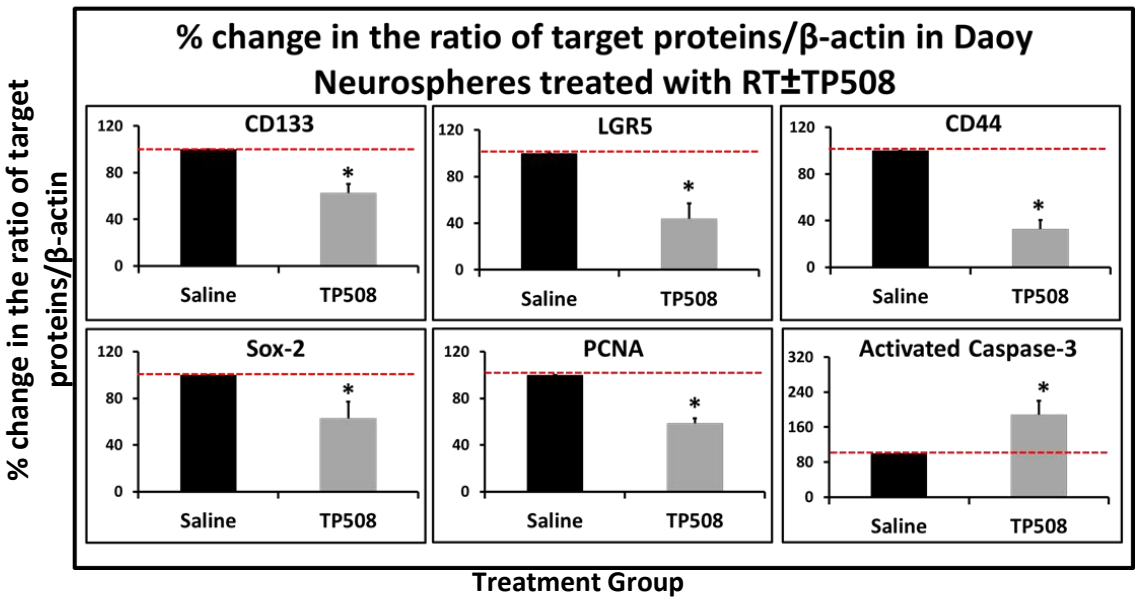

Figure 3.2 Effects of TP508 on stem cell, proliferative, and apoptotic markers

A) Western blot analysis of the indicated markers in Saline vs. TP508 treated Daoy neurospheres collected 4 days post-RT. B) Mean ± standard deviation of Western blot data from 3 experiments, presented as percent change in ratio of target protein/β-actin, from Daoy neurospheres collected 4 days post-RT. Control samples (Saline) were assigned 100 percent values; ratios of TP508 treated groups were expressed as a percent of control. *=P<0.05 vs control.

TP508 decreases the number of cells positive for cancer stem cell markers and proliferation while increasing apoptosis post-RT.

As previously described, Daoy primary neurospheres treated with RT±TP508 were collected at day 4 post-RT. Intact neurospheres were harvested and processed for paraffin embedding using a well-established and published method[100]. Briefly, neurospheres were fixed overnight in 10 percent formalin and re-suspended in 2 percent agar gel containing 0.05 percent sodium azide and stored overnight at 4˚C. After 24 hours, the agar gel containing the neurospheres were paraffin embedded and sections were cut. The sections were probed for cancer stem cell markers, CD133, CD44, LGR5, pluripotent marker, Sox2, proliferative marker, PCNA, and apoptotic marker, activated caspase-3. Results show a significant decrease ($p<0.05$) in the expression levels of all CSC markers, pluripotent marker, Sox2 and proliferative marker, PCNA, in the RT+TP508 treated groups as compared to the RT+saline control (Fig 3.3Ai-ii). On the contrary, the expression levels of activated caspase-3 are significantly ($p<0.05$) increased, indicative of higher cellular death in the TP508 treated neurospheres (Fig 3.3Ai-ii).

Figure 1.3Aiii illustrates the differences in the expression levels of CSC marker CD44 in both unirradiated (0Gy) and irradiated (10Gy) cells, treated plus or minus TP508. Results show that when no radiation is administered and treated plus or minus TP508, CD44 expression is localized throughout the entire sphere. However, upon radiation and saline treatment, expression of CD44 is significantly decreased ($p<0.05$) and remains present in less than 20 percent of the cells located towards the perimeter, where the most resistant stem cells are located[104]. When radiation and TP508 are administered, expression of CD44 is further reduced and is exclusively located on the outer rim of the spheres. The results suggest that radiation alone significantly reduces expression of cancer cells, but adding TP508 pre-radiation synergistically helps decrease cancer cell expression.

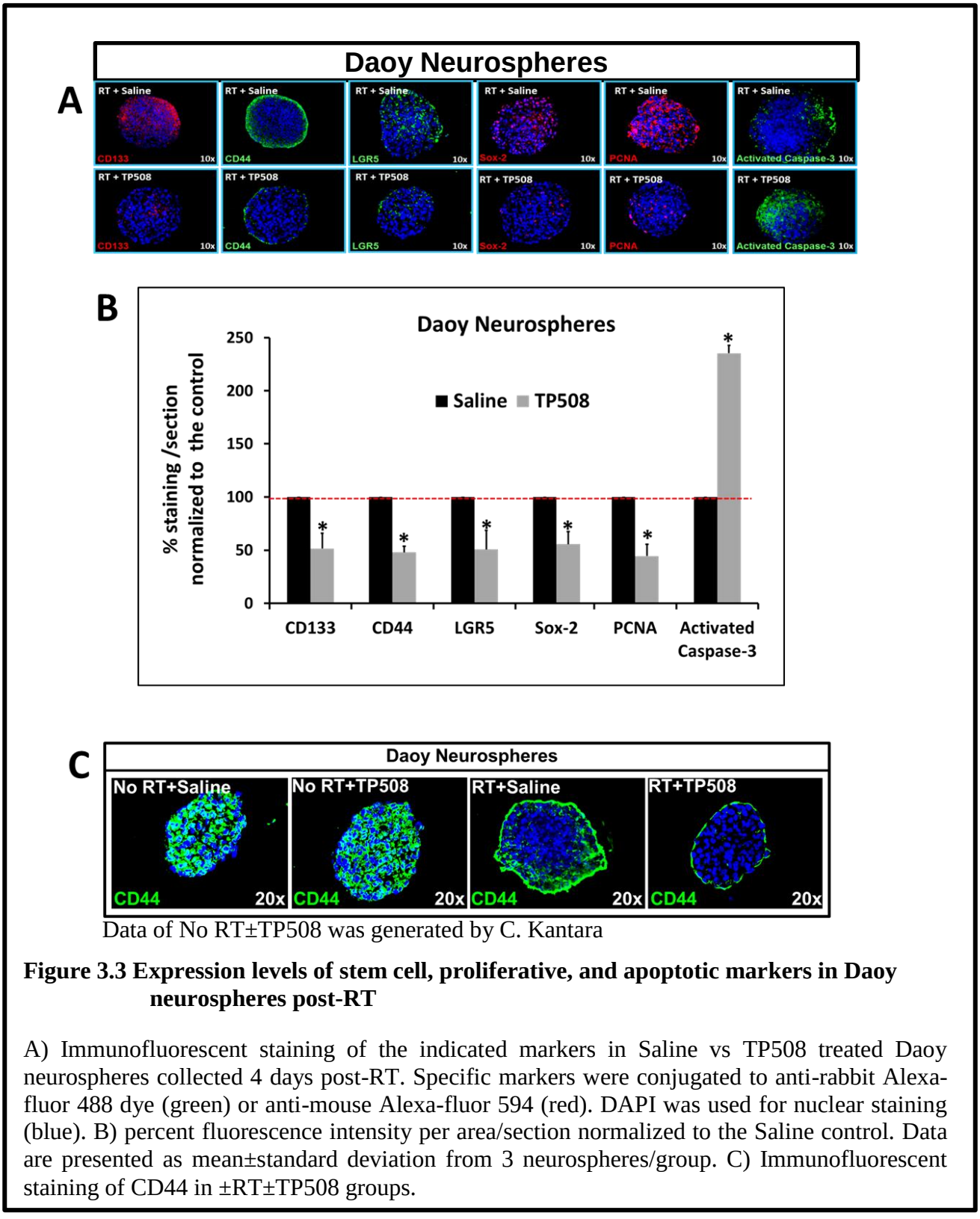

Data of No RT±TP508 was generated by C. Kantara

Figure 3.3 Expression levels of stem cell, proliferative, and apoptotic markers in Daoy neurospheres post-RT

A) Immunofluorescent staining of the indicated markers in Saline vs TP508 treated Daoy neurospheres collected 4 days post-RT. Specific markers were conjugated to anti-rabbit Alexa-fluor 488 dye (green) or anti-mouse Alexa-fluor 594 (red). DAPI was used for nuclear staining (blue). B) percent fluorescence intensity per area/section normalized to the Saline control. Data are presented as mean±standard deviation from 3 neurospheres/group. C) Immunofluorescent staining of CD44 in ±RT±TP508 groups.

Based on these results, I also examined the effects of TP508 treatment on CD133 and CD44 by flow cytometry post-RT (Fig 3.4). Results showed that the expression levels of CD133 and CD44 were significantly decreased by 21 percent (p=0.005) and 26 percent (p=0.03), respectively, as compared to the control. These results were consistent with the Western blot and immunofluorescence data, suggesting that TP508 was sensitizing CSCs and decreasing their stemness potential.

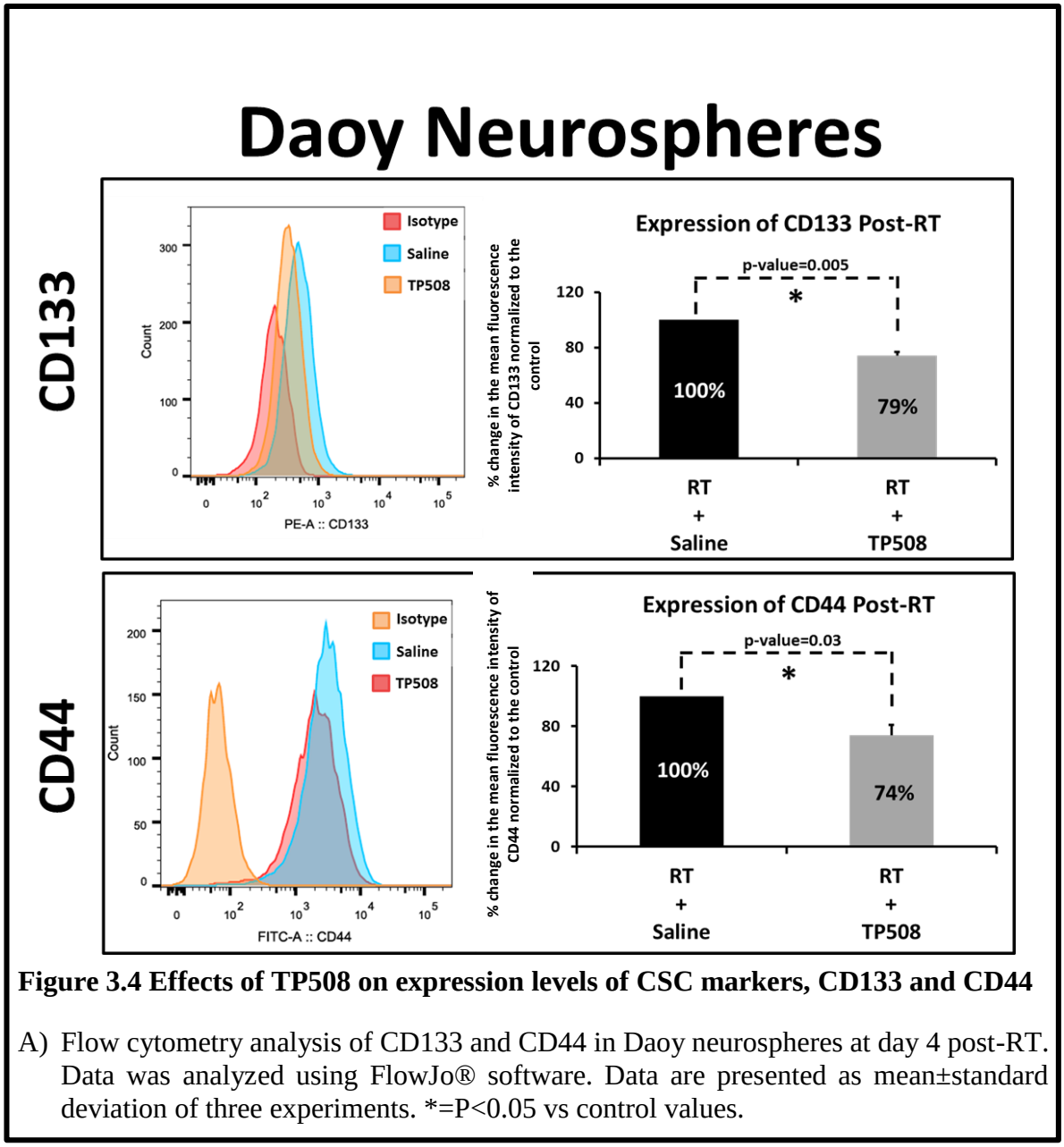

Figure 3.4 Effects of TP508 on expression levels of CSC markers, CD133 and CD44

A) Flow cytometry analysis of CD133 and CD44 in Daoy neurospheres at day 4 post-RT. Data was analyzed using FlowJo® software. Data are presented as mean±standard deviation of three experiments. *=P<0.05 vs control values.

TP508 decreases the tumorigenicity of pre-treated medulloblastoma cancer stem cells in vivo

A study was conducted to examine whether the decrease in cancer stem cell marker expression in medulloblastoma neurospheres by radiation and TP508 treatment would translate into a delay or prevention of tumorigenicity *in vivo*. In these animal experiments, athymic nude mice were inoculated with primary Daoy neurospheres that had been previously treated with saline or TP508 and irradiated with a 0 or 10Gy dose. Neurospheres were collected and mechanically dissociated into single cells 24 hours post-RT and inoculated into the mice at a density of $3x10^6$ cells per flank. Mice were observed 3 times a week for tumor formation. Tumor volume (mm^3) was determined by using the formula ½ (Length × $Width^2$). Results showed that unirradiated cells were the first to start forming a palpable tumor at week 3 post-inoculation (Figure 1.5A). Irradiated cells treated with saline began to form tumors at week 6 post-RT, suggesting that radiation alone delays tumor formation. However, the RT+TP508 treated cells showed the greatest delay in tumor formation, with tumors not forming until week 8 post-RT. Additionally, the weight and size of the RT+TP508 group was decreased as compared to the unirradiated and irradiated control (Fig 3.5Bi-ii). These data suggested that TP508 synergistically decreased cancer cell tumorigenicity and potency. Statistical significance was not tested because the experiment was only conducted once.

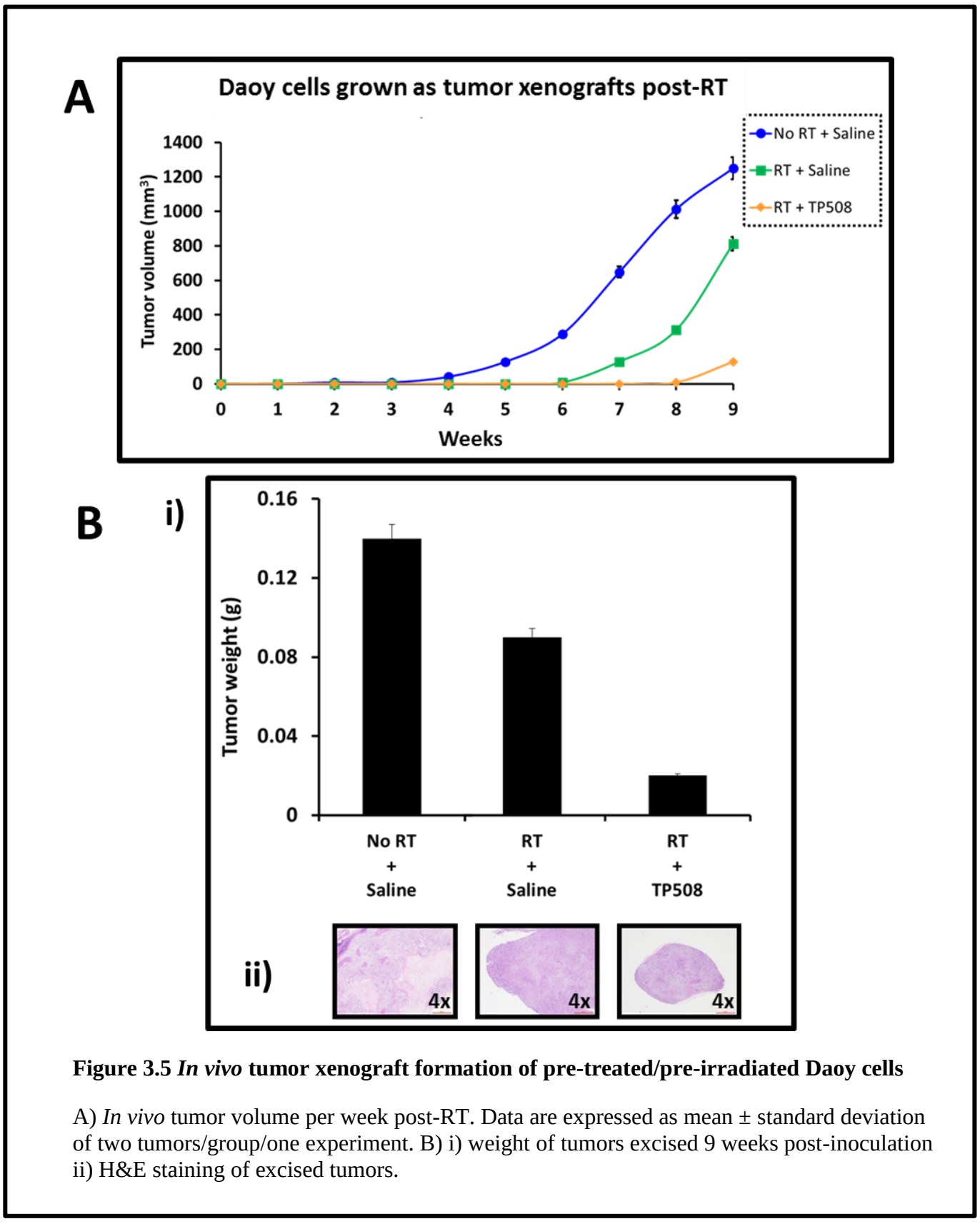

Figure 3.5 *In vivo* tumor xenograft formation of pre-treated/pre-irradiated Daoy cells

A) *In vivo* tumor volume per week post-RT. Data are expressed as mean ± standard deviation of two tumors/group/one experiment. B) i) weight of tumors excised 9 weeks post-inoculation ii) H&E staining of excised tumors.

TP508 decreases the rate of medulloblastoma tumor growth in vivo, post-RT.

Given that TP508 showed radiosensitizing effects *in vitro* it was important to determine whether the peptide would show similar effects when injected in tumor-bearing mice pre-radiation therapy. In this animal model, 5-6 week old athymic nude mice were inoculated in the flanks with untreated monolayer Daoy cells. Tumors were allowed to grow for several weeks until they reached a size of approximately 200mm^3 volume. The mice were then treated with either saline or TP508 (25mg/kg) subcutaneously 1 hour before receiving a 6Gy X-ray radiation treatment localized to the tumor sites. After 23 hours, the mice were treated and irradiated again, for a total TP508 dose of 50mg/kg and a total radiation dose of 12Gy. Tumor volume was monitored 3 times a week. Results showed that there is a significant ($p<0.05$) decrease in tumor growth 2-3 weeks post-RT in the TP508 treated groups as compared to the saline control (Fig 3.6A). Tumors continue to grow in both groups after 1 week of radiation. However, after 1 week post-RT, the saline group tumors continue to grow while the growth in tumors of TP508-treated mice begins to show a downward trend/shrinkage at week 2 post-RT.

Tumors were excised and collected for immunofluorescent staining at week 3 post-RT. Results show a significant decrease ($p<0.05$) in percent staining of CSC markers CD133 and CD44 (Fig 3.6Bi-ii) in the TP508 treated group. The decrease in percent staining was markedly expressed in the borders of the tumors, where resistant cancer stem cells are known to reside[105]. These results were consistent with my *in vitro* data, suggesting that TP508 makes medulloblastoma cancer cells more susceptible to radiation therapy.

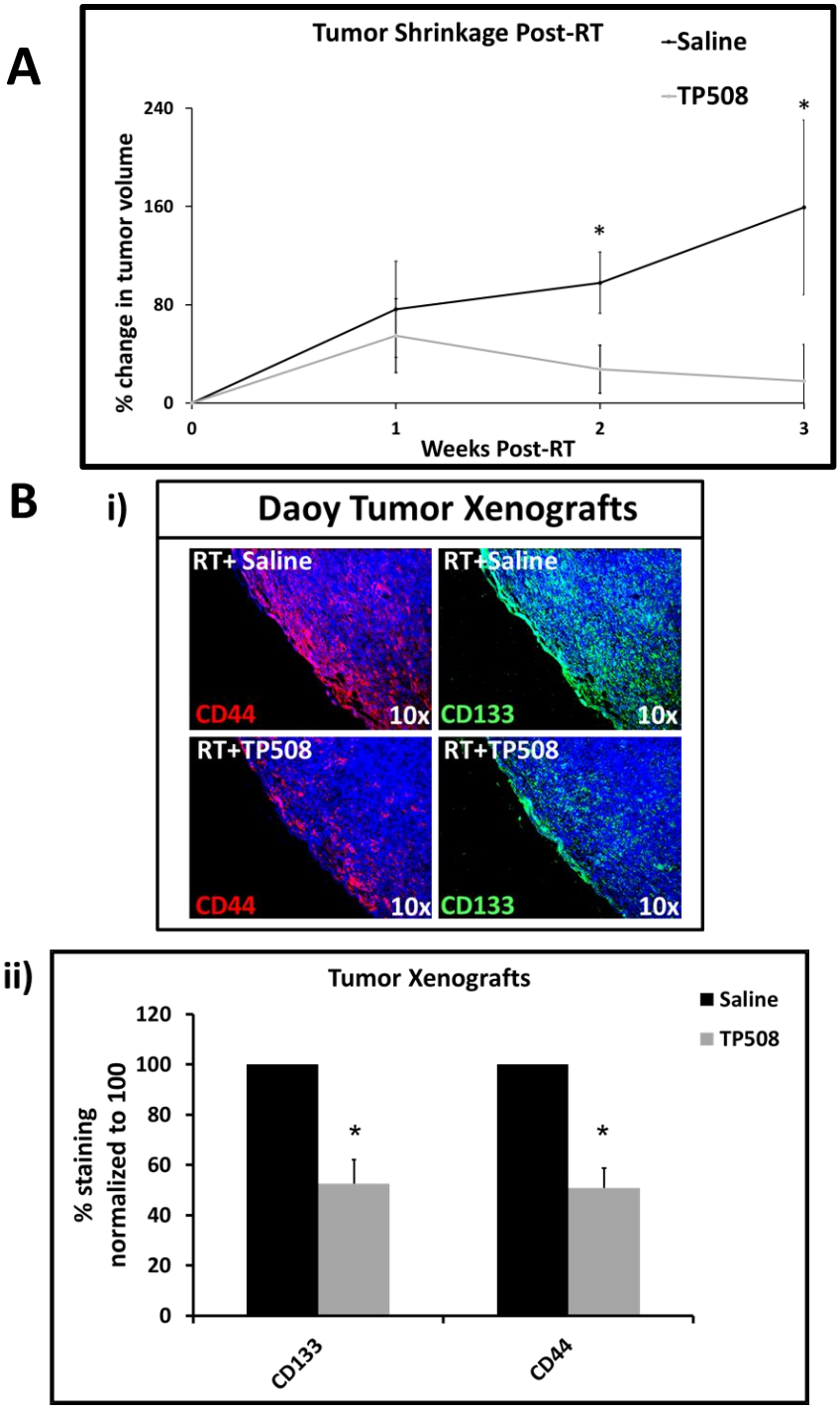

Figure 3.6 Effects of TP508 on Daoy tumor xenografts in athymic nude mice post-RT

A) percent change in tumor volume of tumor xenografts post-RT. Data are presented as mean±standard deviation of three tumors/group/three experiments. *=P<0.05 vs control values. B) i) Immunofluorescent staining of indicated markers in tumors excised 3 weeks post-RT ii) Specific markers were conjugated to anti-rabbit Alexa-fluor 488 dye (green) or anti-mouse Alexa-fluor 594 (red). DAPI was used for nuclear staining (blue). ii) percent fluorescence intensity per area/section normalized to the Saline control. Data are presented as mean±standard deviation from 3 tumors/group.

TP508 effects on cell viability, tumor heterogeneity and relapse potential of glioblastoma cancer stem cells in vitro, post-RT

U-87 MG neurospheres were grown and treated ±TP508 (0.5mg/mL) and exposed to 30Gy of radiation 48h post-treatment. In preliminary studies, the cells were to the same amount of radiation as the Daoy neurospheres (10Gy). However, there were no significant effects of TP508 on cell viability post-radiation. Given that glioblastomas are more malignant than medulloblastomas I hypothesized that perhaps these cells were more resistant to radiation damage and required a higher radiation dose for effects to be observed. Therefore, the radiation dose was increased to 30Gy for studies with the U-87 MG glioblastoma cell line. Neurospheres were dissociated into single cells immediately after radiation, re-seeded, and allowed to re-form as secondary neurospheres. Images were taken daily to assess the ability for the cells to form secondary neurospheres (Fig 3.7 Bi). Results showed no significant differences in the formation of secondary neurospheres or cell viability of TP508 treated neurospheres as compared to the saline control treated neurospheres (Fig 3.7A-Bi-ii). Secondary neurospheres begin to form as early as day 1 post-RT in both the saline and TP508 treated group. Results show that the size (μm) of the secondary neurospheres are also unaffected by TP508 treatment (Fig 3.7Biii).

These findings suggest that TP508 treatment in combination with RT does not exert radiosensitizing effects in the U-87 MG glioblastoma cancer stem cells with this specific treatment protocol. However, it is important to note that although TP508 is not sensitizing the cells to RT it is also not protecting them or increasing their tumorigenic potential.

Overall, the U-87 MG cell line was highly more radioresistant as compared to the Daoy cell line. The cell viability of the U-87 MG cells was 80 percent as compared to a 35 percent in the Daoy cell line in the radiation plus saline treated group. Given that the effects of radiation were not as robust in the U-87 MG cells, it is possible that the cells require a different radiation treatment protocol in order to observe significant effects. To explore this further, future studies should be conducted with fractionated radiation doses in order to

determine whether TP508 may have effects upon this cell line with a more efficient radiation therapy regimen.

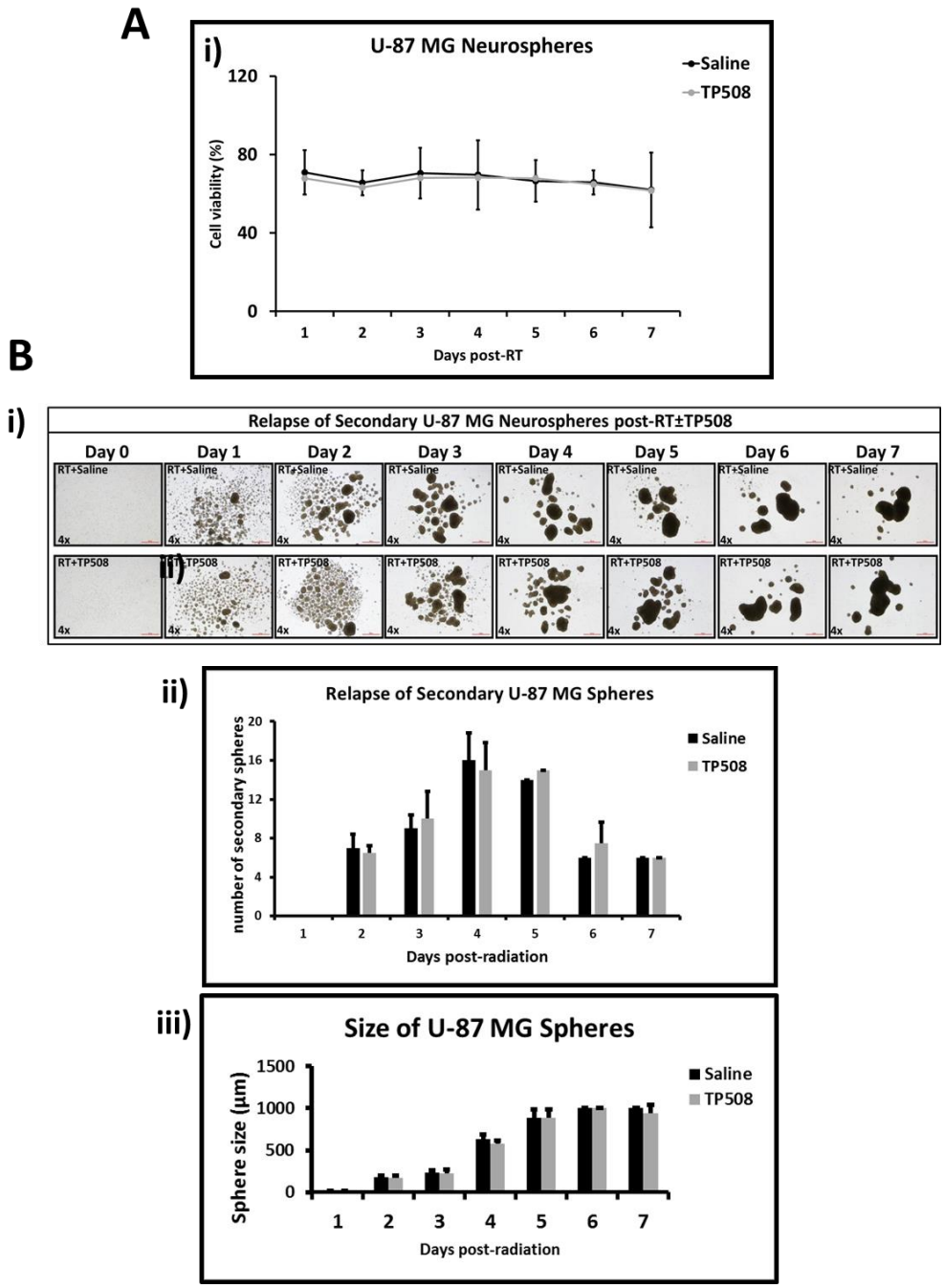

Figure 3.7 Effects of TP508 on U-87 MG spheroidal viability and stemness post-RT

A) Cell viability (percent) of U-87 MG neurospheres post-RT. Data are presented as mean±standard deviation of six wells/day/five experiments. B) i) Representative images taken at 4x of neurospheres dissociated post-RT and re-seeded for secondary neurosphere formation. ii) Bar graph illustrating the number of secondary neurospheres formed post-RT. iii) Bar graph illustrating the size of secondary neurospheres (µm) post-RT. Data are presented as mean±standard deviation of six wells/day/five experiments.

TP508 has no significant effects on proliferation, apoptosis or expression levels of U-87 MG glioblastoma cancer stem cells

U-87 MG neurospheres were treated and irradiated as described above and collected at day 4 post-RT for Western blot analysis. Cell lysates were probed for cancer stem cell markers, CD133, LGR5, CD44, pluripotent marker, Sox2, proliferative marker PCNA, and apoptotic marker, activated caspase-3. Results showed no significant effects of TP508 on the expression of these markers (Fig 3.8A-B). The expression levels of these markers were also examined using immunofluorescent staining of intact U-87 MG neurospheres 4 days post-RT. Results showed no effect of TP508 on any of the indicated markers (Fig 3.9Ai-iii).

In conclusion, TP508 treatment of U87-MG neurospheres prior to radiation did not affect the expression of cancer stem cell and pluripotent markers, nor did it affect their proliferative/apoptotic potential. These results suggest that TP508 does not exert radiosensitizing effects on U-87 MG glioblastoma.

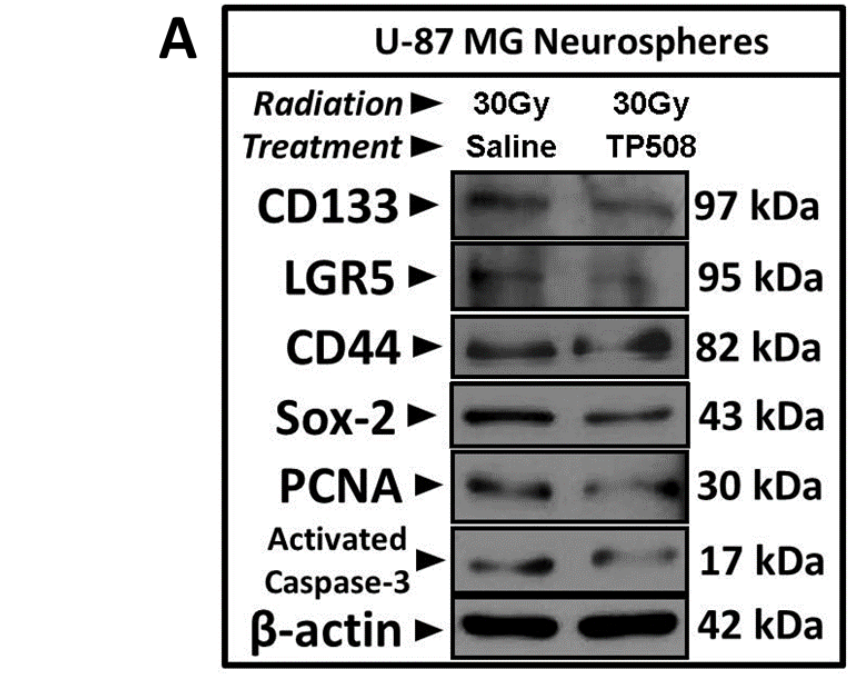

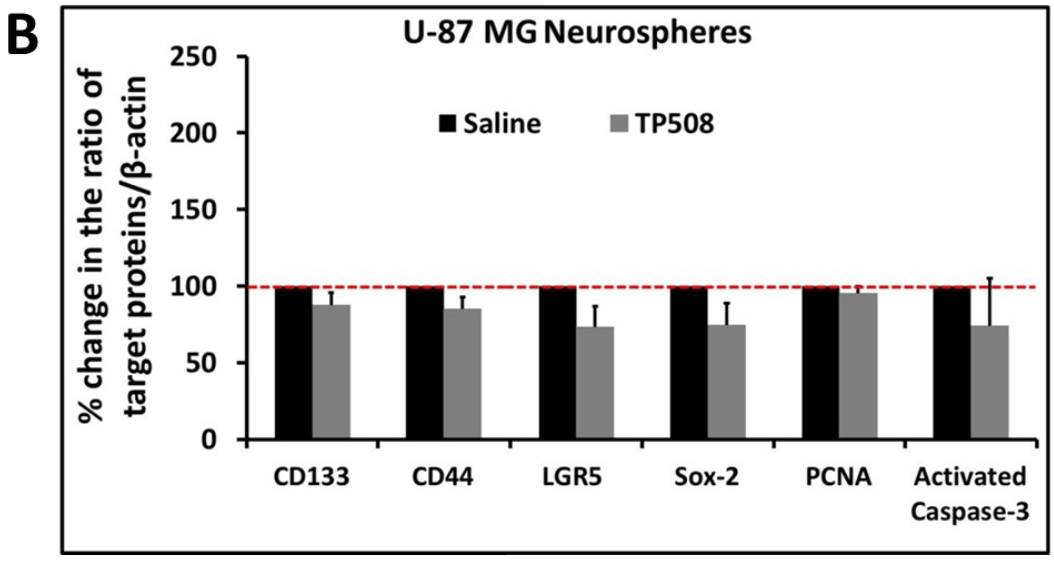

Figure 3.8 Effects of TP508 on U-87 MG stem cell, proliferative, and apoptotic markers post-RT

A) Western blot analysis of the indicated markers in Saline vs. TP508 treated U-87 MG neurospheres collected 4 days post-RT. B) Data are presented as mean ± standard deviation of Western blot data from 3 experiments, presented as percent change in ratio of target protein/β-actin, from neurospheres collected 4 days post-RT. Control samples (Saline) were assigned 100 percent values; ratios of TP508 treated groups were expressed as a percent of control.

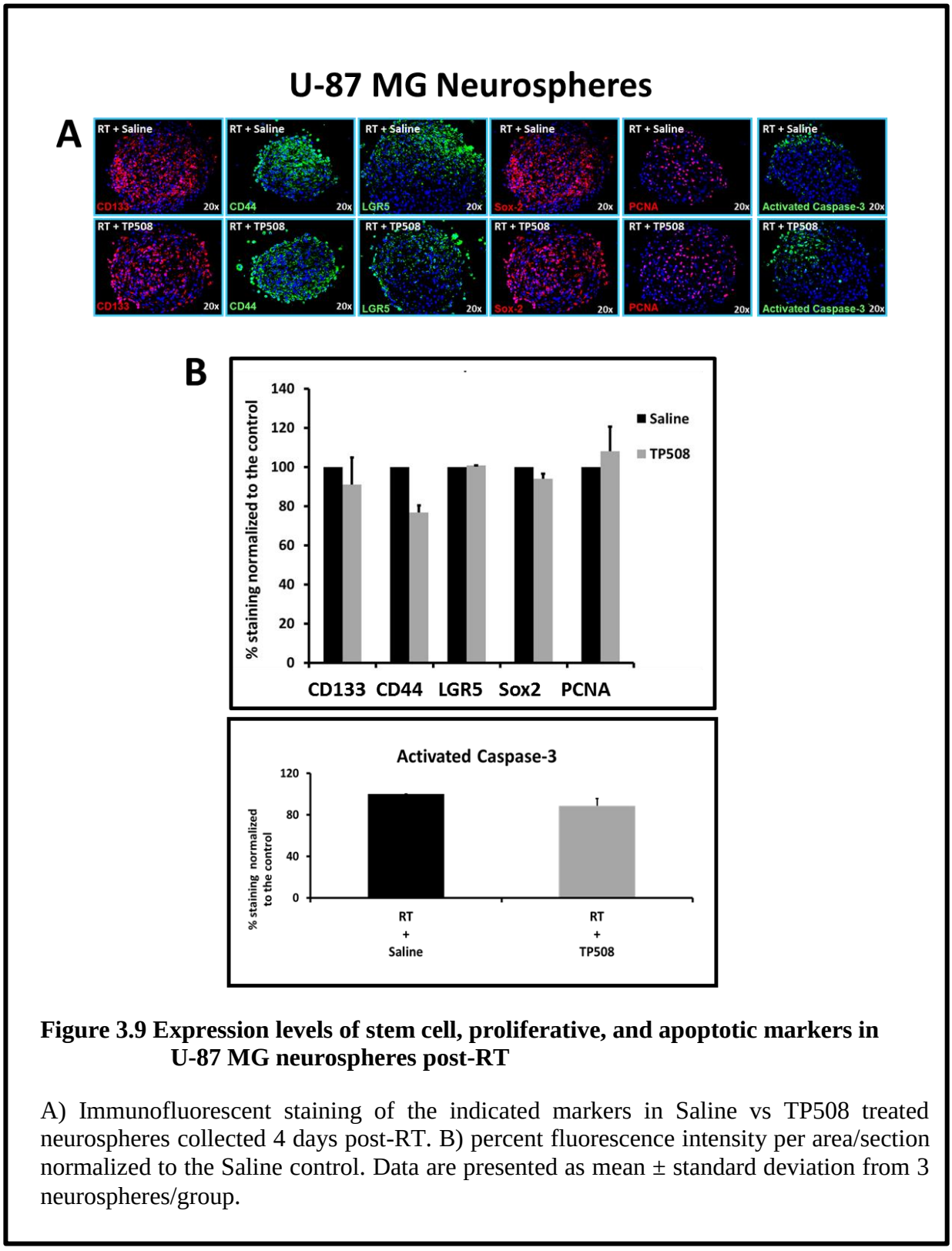

Figure 3.9 Expression levels of stem cell, proliferative, and apoptotic markers in U-87 MG neurospheres post-RT

A) Immunofluorescent staining of the indicated markers in Saline vs TP508 treated neurospheres collected 4 days post-RT. B) percent fluorescence intensity per area/section normalized to the Saline control. Data are presented as mean ± standard deviation from 3 neurospheres/group.

Discussion

In these studies I showed that TP508 treatment of medulloblastoma CSCs significantly radiosensitizes cells and makes them more susceptible to radiation effects. More specifically, my studies showed that TP508 decreased cell viability, tumor heterogeneity, and relapse potential of CSCs in medulloblastoma neurospheres, post-RT (Fig 3.1). Research has shown that spheres are more resistant to radiation therapy due to their rich population of stem and progenitor cells[106]. This suggests that an increase in radiosensitivity within spheres would result in increased spheroidal cell death and decreased capacity to form secondary spheres[107, 108]. My studies show a significant decrease in secondary neurosphere formation in TP508 treated neurospheres as compared to the control, suggesting that TP508 may exert its effects by targeting pathways that are upregulated in CSCs. Studies by Hardee et al.[108], showed that inhibition of certain growth factors significantly decreased the formation of secondary neurospheres in brain cancer cells. Therefore it may be possible that the observed decrease in neurosphere formation was due to a downregulation of growth factors by TP508.

Studies have extensively shown that elevated expression levels of specific CSC markers are associated with a more malignant and tumorigenic phenotype in numerous cancers[109, 110]. Furthermore, inhibition or downregulation of CSC markers, such as CD133, LGR5, and CD44, has been shown to decrease tumor growth and cancer stemness potential[100]. As such, the search for novel and non-toxic CSC targeted therapies have increased over the years. Some of these potential treatment modalities include targeting cell surface markers, utilizing nanoparticle delivery systems, targeting CSC niche microenvironments such as hypoxia, and inducing CSC differentiation to decrease treatment resistance[43, 111]. My studies showed that TP508 significantly decreased the expression levels of CSC markers. CD133, CD44 and LGR5, and proliferative marker, PCNA were decreased, while apoptotic marker, activated caspase-3 was increased in

medulloblastoma CSCs post-RT (Figs. 1.2 and 1.3). This suggests that TP508 may be a potential therapeutic for targeting cancer stem cells.

Targeting signaling pathways known to upregulate CSCs has also shown to sensitize CSCs and render them more susceptible to RT. Youzhi et al., demonstrated that the downregulation of stat inhibitors decreased secondary sphere formation, increased cellular death, inhibited tumor relapse *in vivo*, and decreased expression levels of colon CSC markers[112]. These data suggested that inhibiting key molecules responsible for CSC stemness potential is crucial in targeting these cells[112]. While these studies were not conducted in combination with radiation therapy, they provide evidence that targeting cancer stemness is an effective method in preventing potential tumor relapse. In my studies, TP508 decreased the levels of stem cell markers and medulloblastoma growth relapse, suggesting that TP508 may be targeting key molecules involved in medulloblastoma CSC regulation.

The use of radiosensitizers to specifically target CSCs is also being investigated by several groups. Lagerweij et al. showed that treatment with Quercetin, a flavonoid chemical, significantly radiosensitized SHH and group 3 medulloblastoma subtypes[113]. Results showed that Quercetin treatment pre-RT increased radiosensitivity of the cells, prolonged survival in an orthotopic xenograft mouse model, and decreased cell viability[113]. Given that my studies also showed that TP508 exerts radiosensitizing effects on the SHH medulloblastoma subtype, it may be possible that TP508 also prolongs survival in mice with orthotopic xenografts. Studies will need to be conducted to explore this further.

Although TP508 attenuated tumor growth post-irradiation (Fig1.6), tumors from a mice dosed with TP508 showed tumor relapse 5 weeks post-RT (data not shown). In these cases, the combination of TP508 and radiation may not have been sufficient to totally eradicate the tumors. Because this observation was only seen in a small number of mice, the benefit of tumor volume reduction during the first 3 weeks post-treatment could potentially outweigh the possibility of tumor relapse. It is possible that multiple radiation

and TP508 treatments may be necessary to sustain the observed effects. Therefore, this should be evaluated in a large study before being assessed in clinical trials.

It is important to note that radiosensitizing effects were not observed in U-87 MG glioblastoma cell line. This raises the question as to why the effects were specific to the Daoy medulloblastoma cells. One theory is that TP508 sensitization may be unique to tumor cells with a specific type of mutation in one of the DNA repair enzymes. Another theory may be that TP508 targets specific key molecules in pathways involved in medulloblastoma that are not present in glioblastomas.

CHAPTER 4: EFFECTS OF TP508 ON RADIATION-INDUCED DNA DAMAGE AND DNA DAMAGE REPAIR

Introduction

Results from my *in vitro* and *in vivo* experiments indicate that TP508 sensitizes medulloblastoma cancer stem cells to radiation therapy. Therefore, I sought to determine possible mechanisms by which TP508 exerted these effects, specifically whether TP508 may be exerting its radiosensitizing effects by interfering with DNA damage repair proteins involved in the repair of DNA double-strand break (DSB) repair proteins. Cancer stem cells are particularly adept at surviving radiation-induced damage due to their ability to activate a robust DNA damage repair response (DRR) which allows them to repair DNA double strand breaks (DSBs) more rapidly and thus evade apoptosis[114]. Radiation-induced DNA double-strand breaks activate a damage repair response wherein ATM kinase phosphorylates histone H2AX. Once phosphorylated, the histone is termed gamma-H2AX (γH2AX)[115-117].

Therefore, I first examined the expression levels of γH2AX as a measure of DNA damage post-RT and then examined the roles of non-homologous end joining (NHEJ) and homologous recombination (HR).

Results

TP508 increases the expression of RT-induced DNA double-strand breaks in medulloblastoma cancer stem cells post-RT

To examine the extent of DNA damage post-radiation therapy (RT), Daoy neurospheres treated plus or minus TP508 (0.5 mg/mL) were collected for Western blot analysis, at 1 hour, 4 hours, 24 hours and 72 hours post-RT. Results showed that TP508-treated cells expressed significantly higher levels ($p<0.05$) of DNA DSB marker, γH2AX, in medulloblastoma CSCs at 1-hour post-RT (Fig 4.1A-B). At 4h, the band densities of the TP508 treated groups were also higher, although not statistically significant as compared to the saline control (Fig 4.1A).

Intact Daoy neurospheres were also stained by immunofluorescence 4 days post-RT for the expression of γH2AX marker. γH2AX foci cluster at the sites of DNA DSBs and are dephosphorylated and released upon DNA repair. Thus, the presence of γH2AX is an important marker of DNA DSB repair. Visualizing these foci allows for the quantification of DNA damage by analyzing the percent fluorescence intensity of γH2AX. Results show that TP508 treated neurospheres express significantly higher ($p<0.05$) percent staining of γH2AX in the TP508 vs saline treated groups (Fig 4.2Ai-ii). This was a significant finding, given that even 4 days after radiation, there are a large number of unrepaired DSBs that continue to be expressed in the neurospheres.

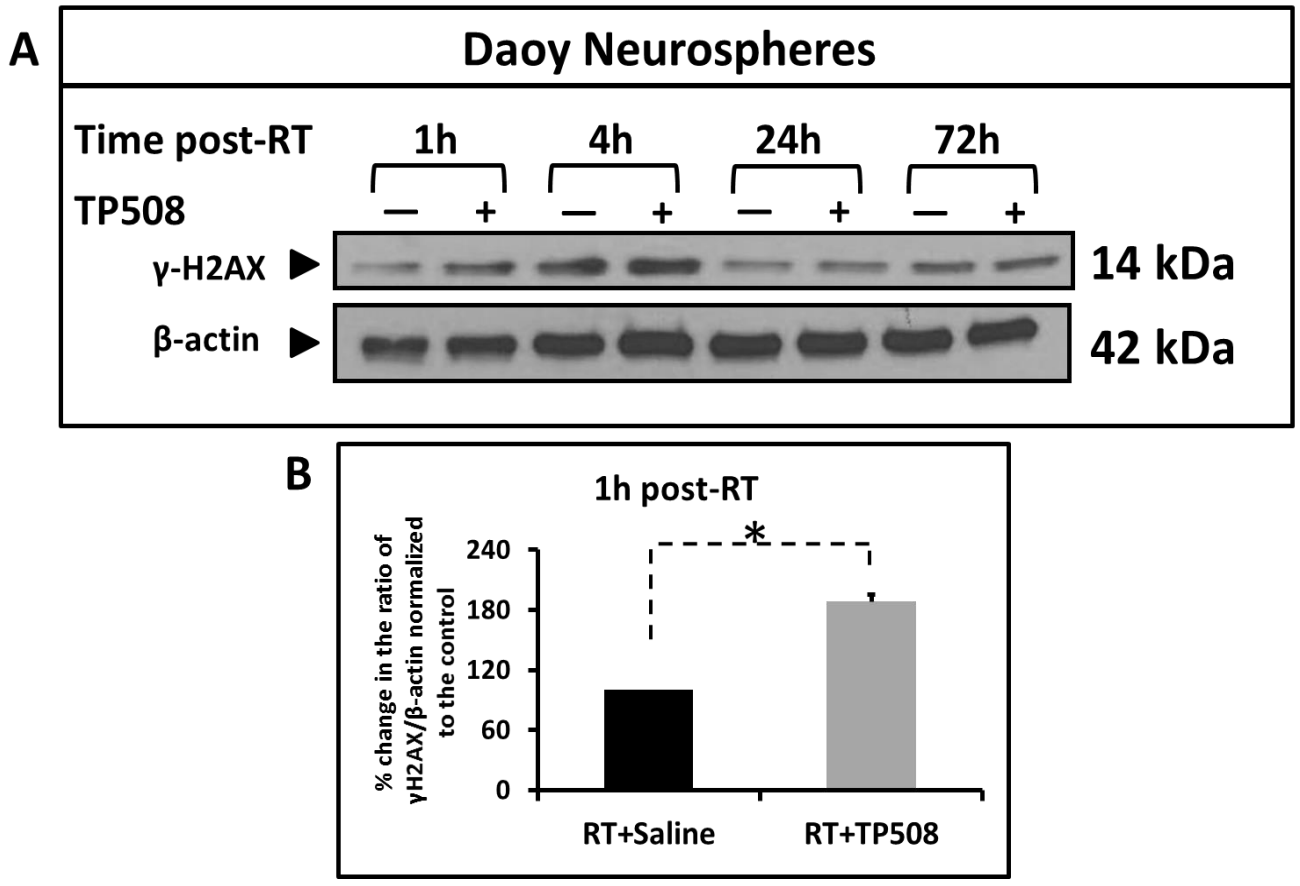

Figure 4.1 Expression level of DNA DSB marker, γH2AX, in Daoy neurospheres post-RT

A) Western blot analysis of γH2AX in Saline vs. TP508 treated Daoy neurospheres collected and lysed at the labeled time-points. B) Data are presented as mean ± standard deviation of Western blot data from 3 experiments presented as percent change in ratio of target protein/β-actin samples (Saline) were assigned 100 percent values; ratios of TP508 treated groups were expressed as a percent of control. *=$P<0.05$ vs control values.

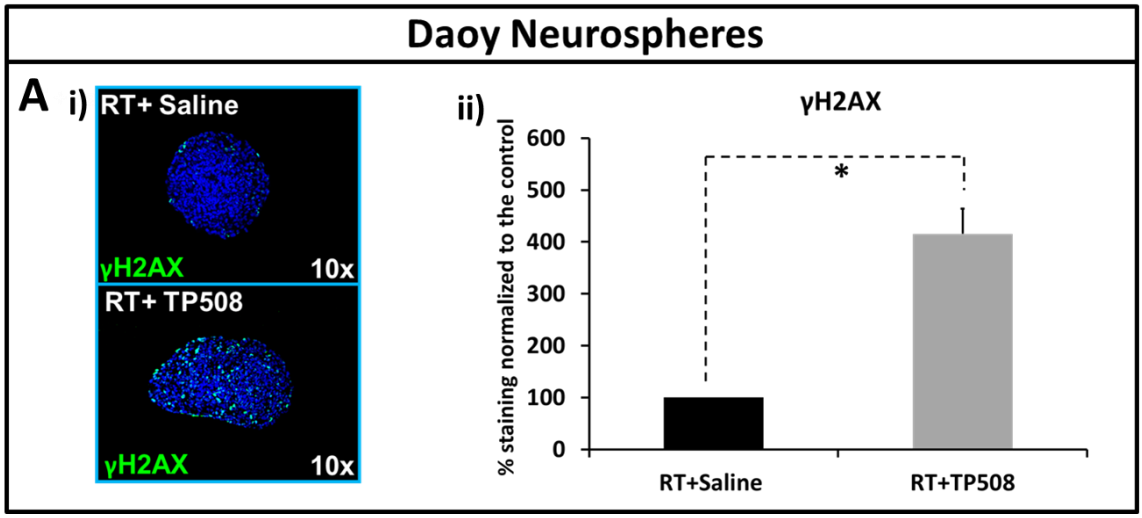

Figure 4.2 Expression level of gamma-H2AX in Daoy neurospheres 4 days post-RT

A i) Immunofluorescent staining of γH2AX in Saline vs TP508 treated neurospheres collected 4 days post-RT. ii) percent staining/section normalized to the Saline control. Data are presented as mean±standard deviation of percent staining of sections from 3 neurospheres/group. *=P<0.05 vs control values.

TP508 does not have an effect on the expression levels of key molecules involved in the non-homologous end joining DNA repair mechanism

After finding that there was delay or inhibition of repair, resulting in higher number of DNA DSBs, in TP508 treated medulloblastoma cancer stem cells, I next examined whether this was due to TP508 inhibiting DNA repair mechanisms.

Daoy neurospheres were treated plus or minus TP508 and irradiated as described in Chapter 3. Cells were collected for Western blot analysis at 1 hour, 4 hours, 24 hours and 72 hours post-RT (Fig 4.3). The cell lysates were probed for DNA Ligase IV and Ku70 which are key molecules involved in non-homologous end joining (NHEJ). Ku70 is an early response sensor and DNA Ligase IV is a late effector of the repair process[73]. Results showed no significant differences in expression levels of these proteins in saline vs TP508 treated neurospheres post-RT. Cells were also collected at earlier time points (0.5 hour, 1 hour, and 2 hours post-RT) and no significant differences were found in the protein expression levels of Ku70, DNA Ligase IV, or XLF, a late effector of NHEJ.

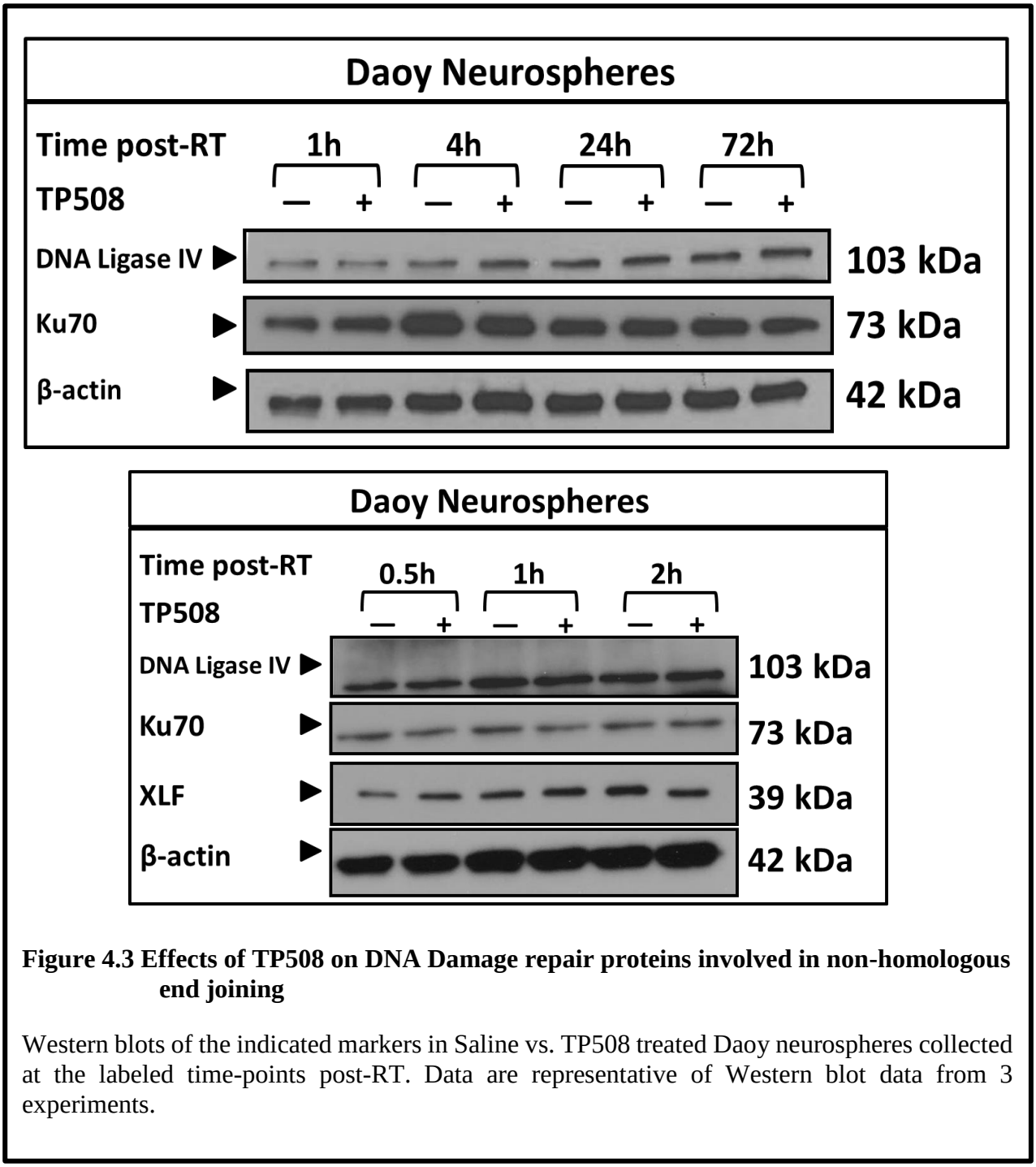

Figure 4.3 Effects of TP508 on DNA Damage repair proteins involved in non-homologous end joining

Western blots of the indicated markers in Saline vs. TP508 treated Daoy neurospheres collected at the labeled time-points post-RT. Data are representative of Western blot data from 3 experiments.

TP508 decreases the expression levels of phosphorylated -BRCA1, a key molecule involved in the homologous recombination DNA repair pathway

As previously discussed, homologous recombination (HR) is a DNA DSB repair pathway that occurs primarily during S or early G2 phase of the cell cycle. For the purpose of these studies, two early response activators of the HR pathway were examined.

Daoy neurospheres were treated plus or minus TP508 and irradiated as described in Chapter 3 and collected for Western blot analysis at 0.5 hour, 1 hour, and 2 hours post-RT (Fig 4.4). The cell lysates were probed for sensors, phosphorylated-BRCA1^{ser1524} and RAD50[73]. Results show that the expression of p-BRCA1^{ser1524} is significantly decreased ($p<0.05$) in the TP508 treated neurospheres 2 hours post-RT (Fig 4.4B). Rad50 is also slightly decreased, although not significantly.

Interestingly, activation of p-BRCA1 not only plays an important role in HR, but it also activates cell cycle checkpoints responsible for arresting the cell cycle to promote DNA repair. It may be possible that there are downstream effects on the regulation of cell cycle activity. Therefore, I next examined the effects of TP508 on cell cycle checkpoint activity post-irradiation.

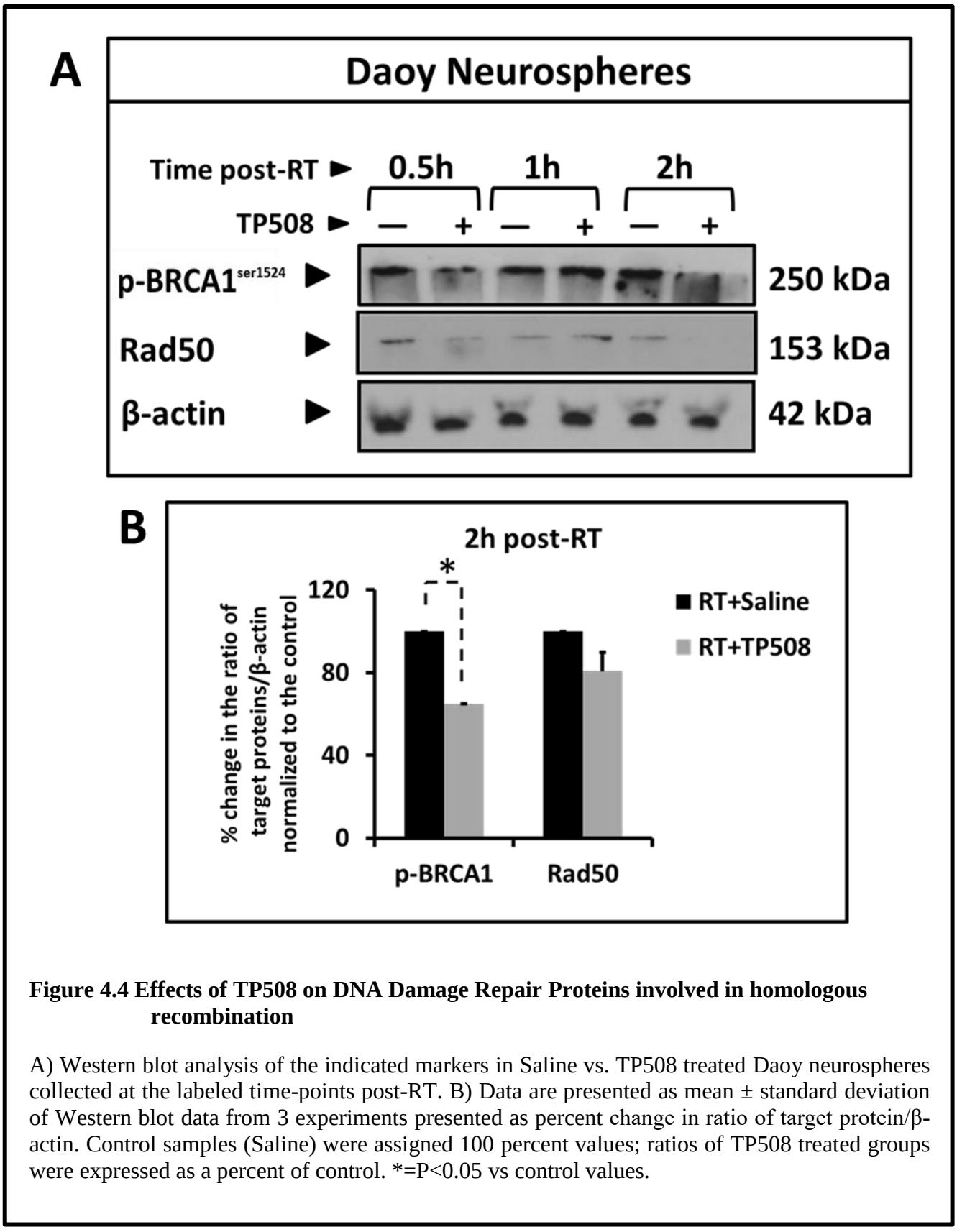

Figure 4.4 Effects of TP508 on DNA Damage Repair Proteins involved in homologous recombination

A) Western blot analysis of the indicated markers in Saline vs. TP508 treated Daoy neurospheres collected at the labeled time-points post-RT. B) Data are presented as mean ± standard deviation of Western blot data from 3 experiments presented as percent change in ratio of target protein/β-actin. Control samples (Saline) were assigned 100 percent values; ratios of TP508 treated groups were expressed as a percent of control. *=$P<0.05$ vs control values.

TP508 decreases the expression levels of cell cycle checkpoints 1 and 2

Cell cycle arrest after radiation-induced DNA damage is an essential step of DNA damage repair and cell survival. The purpose of these experiments was to examine the effects of TP508 on the activation of cell cycle regulators in Daoy medulloblastoma neurospheres post-radiation treatment. Checkpoint kinase 1 and checkpoint kinase 2 are both activated upon radiation damage and in turn activate cell cycle arrest at G2 and G1, respectively in order to promote DNA repair before allowing the cell cycle to progress[118].

Expression levels of phosphorylated-checkpoint kinase 1 (p-Chk1^{Ser345}) and phosphorylated checkpoint kinase 2 (p-Chk2^{Thr68}) begin to decrease in TP508 treated medulloblastoma neurospheres 1 hour post-RT and are significantly decreased as compared to the saline control at 2 hours post-RT ($p<0.05$), (Fig 4.5). These data suggest that TP508 may be preventing or delaying DNA repair by inhibiting cell cycle arrest post-RT.

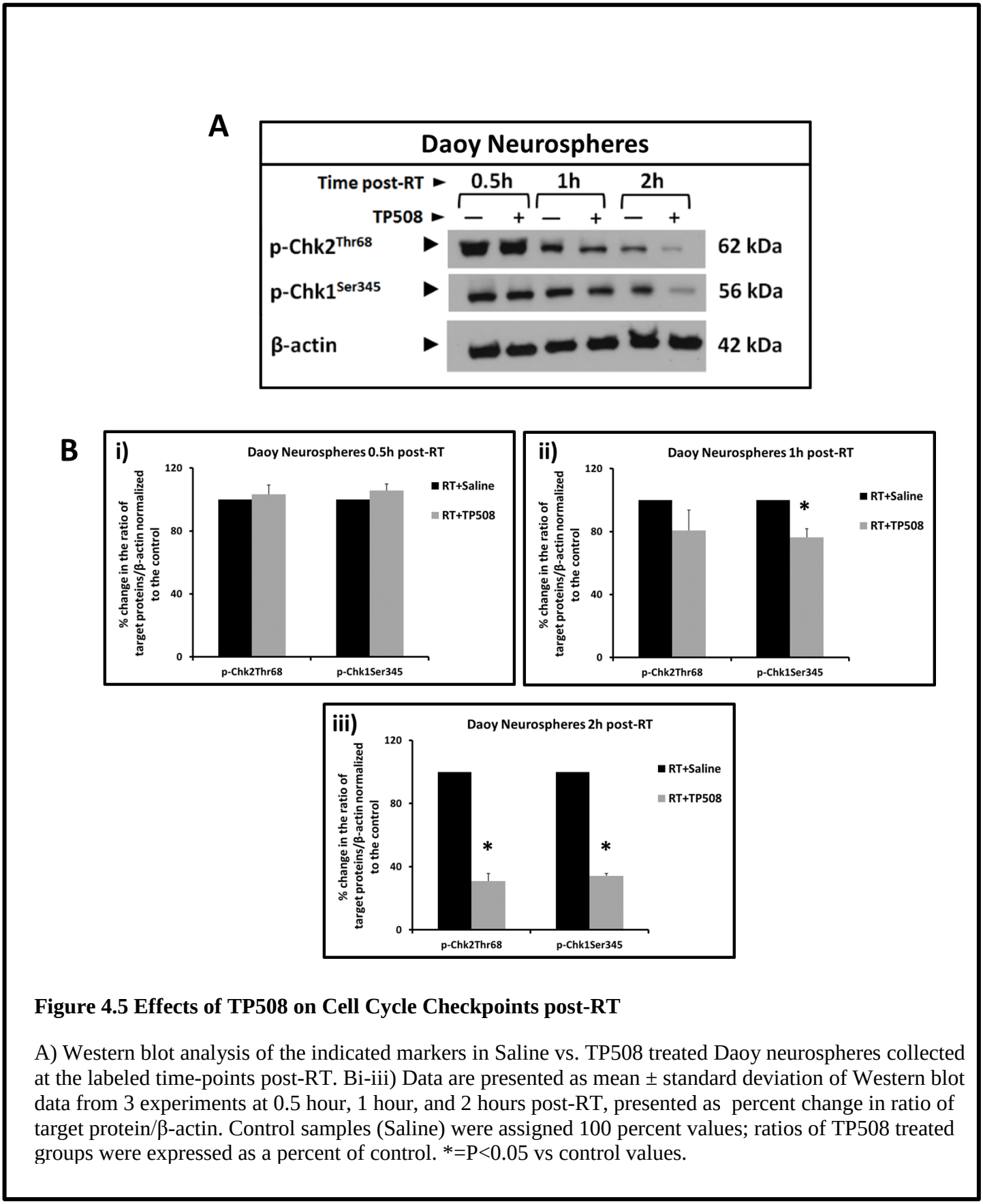

Figure 4.5 Effects of TP508 on Cell Cycle Checkpoints post-RT

A) Western blot analysis of the indicated markers in Saline vs. TP508 treated Daoy neurospheres collected at the labeled time-points post-RT. Bi-iii) Data are presented as mean ± standard deviation of Western blot data from 3 experiments at 0.5 hour, 1 hour, and 2 hours post-RT, presented as percent change in ratio of target protein/β-actin. Control samples (Saline) were assigned 100 percent values; ratios of TP508 treated groups were expressed as a percent of control. *=P<0.05 vs control values.

Discussion

Cancer stem cells (CSCs) are known to have a robust DNA damage repair response that allows them to rapidly repair post-radiation damage. Given that TP508 treatment decreased CSC viability and stemness potential post-radiation therapy (RT), my goal was to examine whether the peptide might be exerting its effects by interfering with DNA damage repair mechanisms.

I first conducted studies to quantify DNA damage post-radiation in control vs TP508 treated neurospheres. I found that the expression of double-strand break marker, γH2AX, was elevated in TP508 treated neurospheres 1-hour post-RT. In studies by Taneja et al., it was shown that cancer cell lines that retained γH2AX foci after an extended period of time post-radiation were more radiosensitive than those that rapidly cleared gamma-H2AX foci[119]. Therefore, residual γH2AX foci are indicative of unrepaired damaged DNA. In my studies, I showed that γH2AX levels were significantly higher in TP508 treated neurospheres, compared to the control, even 4 days post-RT (Fig 4.2). My studies also showed that apoptosis was elevated at day 4 post-RT (Fig 3.2), suggesting that the residual γH2AX-foci staining was due to unrepaired cells that were pushed towards apoptosis. My results are consistent with those of Taneja et al., who similarly found residual γH2AX foci to be an indicator of cellular death in cancer cells post-RT.

Having established that there was an increase in DNA damage in the TP508 vs control groups, I next examined the effects of TP508 on DNA damage repair pathways of non-homologous end joining (NHEJ) and homologous recombination (HR). While I did not find any effects of TP508 on NHEJ molecules, I did find a significant decrease ($p<0.05$) in the phosphorylation of the key HR molecule, BRCA1, 2 hours post-RT. Research has shown that BRCA1 is phosphorylated by ATM at residue serine 1524 during S-phase, which in turn promotes cell cycle arrest by phosphorylating checkpoint kinases[120]. Interestingly, I also found that phosphorylation of checkpoint kinase 1 and checkpoint

kinase 2 were decreased at 2hrs post-RT (Fig 4.5), suggesting that TP508 may be exerting its radiosensitizing effects by inhibiting cell cycle arrest and therefore not allowing the DSB repair process to take place.

Studies show that Chk1 and Chk2 activation is significantly higher in cancer stem cell populations. For instance, CD133-positive ($CD133^{+ve}$) cells express higher levels of activated Chk1 and Chk2 as compared to their CD133-negative ($CD133^{-ve}$) counterparts, making them more radioresistant[118]. Specifically in Daoy medulloblastoma cells, $CD133^{+ve}$ cells were found to be more resistant to sublethal DNA damage compared to the $CD133^{-ve}$ cells[118]. Therefore, decreasing survival of cells expressing CSC markers, such as CD133, within the tumor bulk could be beneficial in inhibiting DNA repair mechanisms. My studies show both a decrease in CSCs and a decrease in checkpoint kinase activity post-RT. Therefore, it is possible that the inhibition of checkpoint kinase activity is responsible for the observed decrease in CSC expression in Chapter 3 studies.

Given their therapeutic potential, checkpoint kinase inhibitors are being investigated as treatment options in various cancer types. Research has shown that Chk1 can be activated by both radiation and chemotherapy induced damage[121]. Specifically in medulloblastoma, the Group 3 subtype has been shown to respond positively to Chk1 inhibitors in combination with the chemotherapeutic agent, cisplatin[122]. Prince et al. conducted studies demonstrating that the addition of Chk1 inhibitors to cisplatin therapy exerted more robust cancer cell killing effects than either treatment alone[122]. Results showed an increase in DNA damage and an induction of apoptosis when treatments were combined. Similarly, my studies showed that TP508 synergistically enhances the effects of radiation, thereby potentiating cellular death. Given that my studies showed checkpoint 1 kinase inhibition in medulloblastoma CSCs, it is possible that the peptide will also exert synergistic effects in combination with chemotherapeutic agents.

Checkpoint kinase 1 inhibitors are also specifically being studied as radiosensitizers given that they can potentially target p53 mutated cancer cells while sparing normal

cells[123]. Normal, p53 wild-type, cells are capable of activating cell cycle arrest at both G2/M and G1 phases[121]. If cells are treated with a G2/M inhibitor, they still have an intact G1 arrest site that can be activated. On the contrary, p53 mutated cells are deficient in activating G1 arrest, and therefore rely solely on G2 arrest for DNA repair. Treating p53 mutated cancer cells with a checkpoint 1 kinase inhibitor would result in its inability to arrest at G2/M, forcing the cell to progress through the cell cycle without repairing, thus inducing apoptosis[124]. Given that I only found significant radiosensitizing effects in the p53 mutated cells (Daoy) and not p53 wild-type cells (U-87 MG) I hypothesized that TP508 may be exerting its effects by inhibiting cell cycle checkpoint activation at G2/M. Although my results showed that there was also inhibition of the G1 checkpoint kinase 2, studies have shown that in some cancer cells Chk2 inhibition alone is insufficient in preventing cell cycle arrest at G1. Therefore, it is possible that U-87 MG have more robust cell cycle arrest mechanisms that overcome TP508 inhibition at G1. To further explore this hypothesis studies would need to be conducted in several p53 WT vs p53 mutated cancer cells. This might help us better understand the mechanisms by which TP508 exerts radioprotectant effects in normal stem cells and radiosensitizing effects in cancer stem cells.

CHAPTER 5: CONCLUSION

Overview

The goal of my dissertation was to examine whether TP508 had any protectant or pro-tumorigenic effects on medulloblastoma and glioblastoma cancer stem cells. To address this goal, I used a spheroidal assay and conducted studies to examine the effects of TP508 on stemness and relapse potential. Results showed that TP508 did not protect medulloblastoma or glioblastoma cells from radiation effects. In fact, TP508 was shown to decrease expression of CSC markers, decrease cell viability of CSCs, and delay tumor relapse of medulloblastoma cells *in vitro* and *in vivo* post-radiation therapy. These studies demonstrated that TP508 sensitized medulloblastoma CSCs to radiation, thereby decreasing their tumorigenic potential.

Based on these findings, my next goal was to examine potential mechanisms by which TP508 may be exerting its radiosensitizing effects. After observing an increase in DNA double-strand breaks (DSBs) in medulloblastoma cells, post-RT, I decided to explore the effects of TP508 on DNA damage repair. Results showed a decrease in the phosphorylation of BRCA1, an important sensor molecule involved in homologous recombination repair and an activator of checkpoint kinases. Additionally, there was a decrease in the activation of cell cycle checkpoints 1 and 2. These studies suggested that TP508 may be exerting the radiosensitizing effects, observed in Chapter 3, by inhibiting cell cycle arrest and therefore not allowing the DSB repair process to take place.

Clinical Relevance

The ability for TP508 to target cancer cells while protecting neuronal cells would make this drug an ideal candidate for the development of a novel non-toxic radiosensitizing agent for cancers. Moreover, development of TP058 may serve a dual role as a novel

radiosensitizer to help prevent recurrence of the disease, and also as a radioprotectant, to spare normal neuronal cells from damage and thereby attenuate cognitive dysfunction. As adjuvant therapy, TP508 could also be beneficial in reducing the radiation dose necessary to achieve optimal therapeutic results, thereby also aiding in preventing radiation-induced cognitive dysfunction.

Study Limitations

One of the limitations of this study is that the experimental design consisted of a single dose or injection of TP508 in the *in vitro* and *in vivo* studies, respectively. In the *in vitro* studies results showed a decrease in cell viability at 3-4 days post-radiation treatment and in the *in vivo* studies results showed an attenuation of tumor growth 3 weeks post-RT. Therefore, it is important to investigate whether or not multiple radiation and TP508 doses would prolong these effects and promote complete tumor elimination. Furthermore, my *in vivo* studies consisted of two fractionated doses of 6Gy, rather than a true clinical model which would require 1.8Gy fractionated doses over the course of several weeks. The athymic nude mouse model limits my ability to test a fractionated dosing regimen similar to those administered in patients given that the mice would most likely not survive treatment. Conducting these studies would help determine if TP508 should optimally be administered weekly, biweekly or perhaps even 1 hour before each radiation dose. Additionally, the studies conducted in this dissertation required a high dose of radiation (10Gy) because CSCs are more resistant to radiation effects. Therefore, studying the effects of TP508 in a heterogenous population of cancer cells in combination with smaller doses of radiation (<10Gy) would help elucidate its potential radiosensiziting effects in a more clinically relevant model.

An additional limitation is that I was unable to study the effects of TP508 on other medulloblastoma subtypes given that there were technical issues with growing and expanding the commercially available cell lines for other subtypes. Studies should be

conducted to examine the effects of TP508 on other medulloblastoma subtypes, particularly Group C, given that it has the worst prognosis.

Future Directions

In this body of work, I have identified mechanisms by which TP508 regulates medulloblastoma CSCs post-radiation treatment. However, there are other essential molecules and pathways involved in medulloblastoma CSC RT resistance, such as the Wnt and nuclear factor NF-κB pathways, which may need to be studied to further elucidate the mode of action of TP508. This could help increase our understanding of how this novel peptide serves a dual role as a radioprotectant of normal stem cells and a radiosensitizer of cancer stem cells.

Additionally, several questions remain to be answered regarding the difference in treatment response observed in the medulloblastoma Daoy cell line and the glioblastoma U-87 MG cell line. Future experiments will need to be conducted to examine the specificity of TP508 in regards to other medulloblastoma subtypes and other brain cancer types. It is possible that in other types of cancers, multiple and/or higher TP508 doses may be necessary for effects to take place. Additionally, it is possible that TP508 may need to be used in combination with other therapeutics, such as chemotherapy, to exert effects on more aggressive cancer types.

Pursuing future studies to address these concerns would offer valuable insight into the potential of TP508 as a novel non-toxic therapeutic to target certain types of brain cancers, improve clinical outcome, and prevent tumor relapse.

REFERENCES

1. Kantara C. Growth factors up-regulate epithelial stem cells: Treatment strategies for colorectal cancers. ProQuest. 2012.

2. Carney D, Kantara, Carla, Moya, Stephanie Methods of Using Thrombin Derivatives to Treat Medulloblastoma. United States, 2015.

3. Society AC. Cancer Facts & Figures 2016. Atlanta: American Cancer Society. 2016.

4. Brandao LA, Young Poussaint T. Posterior Fossa Tumors. Neuroimaging Clin N Am. 2017;27: 1-37.

5. Polkinghorn WR, Tarbell NJ. Medulloblastoma: tumorigenesis, current clinical paradigm, and efforts to improve risk stratification. Nat Clin Pract Oncol. 2007;4: 295-304.

6. Taylor MD, Northcott PA, Korshunov A, et al. Molecular subgroups of medulloblastoma: the current consensus. Acta Neuropathol. 2012;123: 465-472.

7. Srinivasan VM, Ghali MG, North RY, Boghani Z, Hansen D, Lam S. Modern management of medulloblastoma: Molecular classification, outcomes, and the role of surgery. Surg Neurol Int. 2016;7: S1135-S1141.

8. Eberhart CG, Burger PC. Anaplasia and grading in medulloblastomas. Brain Pathol. 2003;13: 376-385.

9. Brun SN, Markant SL, Esparza LA, et al. Survivin as a therapeutic target in Sonic hedgehog-driven medulloblastoma. Oncogene. 2014;0.

10. Matsuo S, Takahashi M, Inoue K, et al. Inhibitory potential of postnatal treatment with cyclopamine, a hedgehog signaling inhibitor, on medulloblastoma development in Ptch1 heterozygous mice. Toxicol Pathol. 2014;42: 1174-1187.

11. Baryawno N, Sveinbjornsson B, Eksborg S, Chen CS, Kogner P, Johnsen JI. Small-molecule inhibitors of phosphatidylinositol 3-kinase/Akt signaling inhibit Wnt/beta-catenin pathway cross-talk and suppress medulloblastoma growth. Cancer Res. 2010;70: 266-276.

12. Martirosian V, Chen TC, Lin M, Neman J. Medulloblastoma initiation and spread: Where neurodevelopment, microenvironment and cancer cross pathways. J Neurosci Res. 2016;94: 1511-1519.

13. Wang VY, Zoghbi HY. Genetic regulation of cerebellar development. Nat Rev Neurosci. 2001;2: 484-491.

14. Hope KJ, Jin L, Dick JE. Acute myeloid leukemia originates from a hierarchy of leukemic stem cell classes that differ in self-renewal capacity. Nat Immunol. 2004;5: 738-743.

15. Childhood Central Nervous System Embryonal Tumors Treatment (PDQ(R)): Health Professional Version. PDQ Cancer Information Summaries. Bethesda (MD), 2002.

16. Adamski J, Ramaswamy V, Huang A, Bouffet E. Advances in managing medulloblastoma and intracranial primitive neuro-ectodermal tumors. F1000Prime Rep. 2014;6: 56.

17. Khatua S. Evolving molecular era of childhood medulloblastoma: time to revisit therapy. Future Oncol. 2016;12: 107-117.

18. Coluccia D, Figuereido C, Isik S, Smith C, Rutka JT. Medulloblastoma: Tumor Biology and Relevance to Treatment and Prognosis Paradigm. Curr Neurol Neurosci Rep. 2016;16: 43.

19. Massimino M, Biassoni V, Gandola L, et al. Childhood medulloblastoma. Crit Rev Oncol Hematol. 2016;105: 35-51.

20. Gopalakrishnan V, Tao RH, Dobson T, Brugmann W, Khatua S. Medulloblastoma development: tumor biology informs treatment decisions. CNS Oncol. 2015;4: 79-89.

21. Khakban A, Mohammadi T, Lynd LD, et al. Societal preferences in the treatment of pediatric medulloblastoma: Balancing risk of death and quality of life. Pediatr Blood Cancer. 2016.

22. Gajjar A, Chintagumpala M, Ashley D, et al. Risk-adapted craniospinal radiotherapy followed by high-dose chemotherapy and stem-cell rescue in children with newly diagnosed medulloblastoma (St Jude Medulloblastoma-96): long-term results from a prospective, multicentre trial. Lancet Oncol. 2006;7: 813-820.

23. Michiels EM, Schouten-Van Meeteren AY, Doz F, Janssens GO, van Dalen EC. Chemotherapy for children with medulloblastoma. Cochrane Database Syst Rev. 2015;1: CD006678.

24. Packer RJ, Gajjar A, Vezina G, et al. Phase III study of craniospinal radiation therapy followed by adjuvant chemotherapy for newly diagnosed average-risk medulloblastoma. J Clin Oncol. 2006;24: 4202-4208.

25. Gajjar AJ, Robinson GW. Medulloblastoma-translating discoveries from the bench to the bedside. Nat Rev Clin Oncol. 2014;11: 714-722.

26. Castelo-Branco P, Tabori U. Promises and challenges of exhausting pediatric neural cancer stem cells. Pediatr Res. 2012;71: 523-528.

27. Hladik D, Tapio S. Effects of ionizing radiation on the mammalian brain. Mutat Res. 2016;770: 219-230.

28. Tang FR, Loke WK, Khoo BC. Postnatal irradiation-induced hippocampal neuropathology, cognitive impairment and aging. Brain Dev. 2016.

29. Agbahiwe H, Rashid A, Horska A, et al. A prospective study of cerebral, frontal lobe, and temporal lobe volumes and neuropsychological performance in children with primary brain tumors treated with cranial radiation. Cancer. 2016.

30. Li MD, Forkert ND, Kundu P, et al. Brain Perfusion and Diffusion Abnormalities in Children Treated for Posterior Fossa Brain Tumors. J Pediatr. 2017.

31. Zeltzer PM, Boyett JM, Finlay JL, et al. Metastasis stage, adjuvant treatment, and residual tumor are prognostic factors for medulloblastoma in children: conclusions from the Children's Cancer Group 921 randomized phase III study. J Clin Oncol. 1999;17: 832-845.

32. Kadota RP, Mahoney DH, Doyle J, et al. Dose intensive melphalan and cyclophosphamide with autologous hematopoietic stem cells for recurrent medulloblastoma or germinoma. Pediatr Blood Cancer. 2008;51: 675-678.

33. Pizer B, Donachie PH, Robinson K, et al. Treatment of recurrent central nervous system primitive neuroectodermal tumours in children and adolescents: results of a Children's Cancer and Leukaemia Group study. Eur J Cancer. 2011;47: 1389-1397.

34. Cloughesy TF, Cavenee WK, Mischel PS. Glioblastoma: from molecular pathology to targeted treatment. Annu Rev Pathol. 2014;9: 1-25.

35. Wen PY, Kesari S. Malignant gliomas in adults. N Engl J Med. 2008;359: 492-507.

36. Omuro A, DeAngelis LM. Glioblastoma and other malignant gliomas: a clinical review. JAMA. 2013;310: 1842-1850.

37. Wurth R, Barbieri F, Florio T. New molecules and old drugs as emerging approaches to selectively target human glioblastoma cancer stem cells. Biomed Res Int. 2014;2014: 126586.

38. Jacobsen PF, Jenkyn DJ, Papadimitriou JM. Establishment of a human medulloblastoma cell line and its heterotransplantation into nude mice. J Neuropathol Exp Neurol. 1985;44: 472-485.

39. Allen M, Bjerke M, Edlund H, Nelander S, Westermark B. Origin of the U87MG glioma cell line: Good news and bad news. Sci Transl Med. 2016;8: 354re353.

40. Jung Y, Kim WY. Cancer stem cell targeting: Are we there yet? Arch Pharm Res. 2015.

41. Gasch C, Ffrench B, O'Leary JJ, Gallagher MF. Catching moving targets: cancer stem cell hierarchies, therapy-resistance & considerations for clinical intervention. Mol Cancer. 2017;16: 43.

42. Botelho M, Alves H. Significance of Cancer Stem Cells in Anti-Cancer Therapies. Int J Immunother Cancer Res. 2016;2: 14-16.

43. Dragu DL, Necula LG, Bleotu C, Diaconu CC, Chivu-Economescu M. Therapies targeting cancer stem cells: Current trends and future challenges. World J Stem Cells. 2015;7: 1185-1201.

44. Holohan C, Van Schaeybroeck S, Longley DB, Johnston PG. Cancer drug resistance: an evolving paradigm. Nat Rev Cancer. 2013;13: 714-726.

45. Li L, Borodyansky L, Yang Y. Genomic instability en route to and from cancer stem cells. Cell Cycle. 2009;8: 1000-1002.

46. Rapp UR, Ceteci F, Schreck R. Oncogene-induced plasticity and cancer stem cells. Cell Cycle. 2008;7: 45-51.

47. Visvader JE, Lindeman GJ. Cancer stem cells in solid tumours: accumulating evidence and unresolved questions. Nat Rev Cancer. 2008;8: 755-768.

48. Yoshii T, Geng Y, Le ND, Goel HL, Mercurio AM, Rotello VM. Highlights from the latest articles in nanomaterial-based therapies for targeting cancer stem cells. Nanomedicine (Lond). 2015;10: 3427-3429.

49. Uchida N, Buck DW, He D, et al. Direct isolation of human central nervous system stem cells. Proc Natl Acad Sci U S A. 2000;97: 14720-14725.

50. Arndt K, Grinenko T, Mende N, et al. CD133 is a modifier of hematopoietic progenitor frequencies but is dispensable for the maintenance of mouse hematopoietic stem cells. Proc Natl Acad Sci U S A. 2013;110: 5582-5587.

51. Ding BS, James D, Iyer R, et al. Prominin 1/CD133 endothelium sustains growth of proneural glioma. PLoS One. 2013;8: e62150.

52. Cheng JX, Liu BL, Zhang X. How powerful is CD133 as a cancer stem cell marker in brain tumors? Cancer Treat Rev. 2009;35: 403-408.

53. Singh SK, Clarke ID, Hide T, Dirks PB. Cancer stem cells in nervous system tumors. Oncogene. 2004;23: 7267-7273.

54. Singh SK, Hawkins C, Clarke ID, et al. Identification of human brain tumour initiating cells. Nature. 2004;432: 396-401.

55. Ponta H, Sherman L, Herrlich PA. CD44: from adhesion molecules to signalling regulators. Nat Rev Mol Cell Biol. 2003;4: 33-45.

56. Haraguchi N, Ohkuma M, Sakashita H, et al. CD133+CD44+ population efficiently enriches colon cancer initiating cells. Ann Surg Oncol. 2008;15: 2927-2933.

57. Al-Hajj M, Wicha MS, Benito-Hernandez A, Morrison SJ, Clarke MF. Prospective identification of tumorigenic breast cancer cells. Proc Natl Acad Sci U S A. 2003;100: 3983-3988.

58. Harabin-Slowinska M, Slowinski J, Konecki J, Mrowka R. Expression of adhesion molecule CD44 in metastatic brain tumors. Folia Neuropathol. 1998;36: 179-184.

59. Patrawala L, Calhoun T, Schneider-Broussard R, et al. Highly purified CD44+ prostate cancer cells from xenograft human tumors are enriched in tumorigenic and metastatic progenitor cells. Oncogene. 2006;25: 1696-1708.

60. Merzak A, Koocheckpour S, Pilkington GJ. CD44 mediates human glioma cell adhesion and invasion in vitro. Cancer Res. 1994;54: 3988-3992.

61. Marangoni E, Lecomte N, Durand L, et al. CD44 targeting reduces tumour growth and prevents post-chemotherapy relapse of human breast cancers xenografts. Br J Cancer. 2009;100: 918-922.

62. Carmon KS, Lin Q, Gong X, Thomas A, Liu Q. LGR5 interacts and cointernalizes with Wnt receptors to modulate Wnt/beta-catenin signaling. Mol Cell Biol. 2012;32: 2054-2064.

63. May R, Sureban SM, Hoang N, et al. Doublecortin and CaM kinase-like-1 and leucine-rich-repeat-containing G-protein-coupled receptor mark quiescent and cycling intestinal stem cells, respectively. Stem Cells. 2009;27: 2571-2579.

64. Nakata S, Campos B, Bageritz J, et al. LGR5 is a marker of poor prognosis in glioblastoma and is required for survival of brain cancer stem-like cells. Brain Pathol. 2013;23: 60-72.

65. Amsterdam A, Raanan C, Schreiber L, Polin N, Givol D. LGR5 and Nanog identify stem cell signature of pancreas beta cells which initiate pancreatic cancer. Biochem Biophys Res Commun. 2013;433: 157-162.

66. Whittier KL, Boese EA, Gibson-Corley KN, et al. G-protein coupled receptor expression patterns delineate medulloblastoma subgroups. Acta Neuropathol Commun. 2013;1: 66.

67. Zhang S, Cui W. Sox2, a key factor in the regulation of pluripotency and neural differentiation. World J Stem Cells. 2014;6: 305-311.

68. Vanner RJ, Remke M, Gallo M, et al. Quiescent sox2(+) cells drive hierarchical growth and relapse in sonic hedgehog subgroup medulloblastoma. Cancer Cell. 2014;26: 33-47.

69. Ahlfeld J, Favaro R, Pagella P, Kretzschmar HA, Nicolis S, Schuller U. Sox2 requirement in sonic hedgehog-associated medulloblastoma. Cancer Res. 2013;73: 3796-3807.

70. Cox JL, Wilder PJ, Desler M, Rizzino A. Elevating SOX2 levels deleteriously affects the growth of medulloblastoma and glioblastoma cells. PLoS One. 2012;7: e44087.

71. Rycaj K, Tang DG. Cancer stem cells and radioresistance. Int J Radiat Biol. 2014;90: 615-621.

72. Aparicio T, Baer R, Gautier J. DNA double-strand break repair pathway choice and cancer. DNA Repair (Amst). 2014;19: 169-175.

73. Raleigh DR, Haas-Kogan DA. Molecular targets and mechanisms of radiosensitization using DNA damage response pathways. Future Oncol. 2013;9: 219-233.

74. Marnef A, Legube G. Organizing DNA repair in the nucleus: DSBs hit the road. Curr Opin Cell Biol. 2017;46: 1-8.

75. Sage E, Shikazono N. Radiation-induced clustered DNA lesions: Repair and mutagenesis. Free Radic Biol Med. 2016.

76. Centurione L, Aiello FB. DNA Repair and Cytokines: TGF-beta, IL-6, and Thrombopoietin as Different Biomarkers of Radioresistance. Front Oncol. 2016;6: 175.

77. Chakraborty A, Tapryal N, Venkova T, et al. Classical non-homologous end-joining pathway utilizes nascent RNA for error-free double-strand break repair of transcribed genes. Nat Commun. 2016;7: 13049.

78. Blanpain C, Mohrin M, Sotiropoulou PA, Passegue E. DNA-damage response in tissue-specific and cancer stem cells. Cell Stem Cell. 2011;8: 16-29.

79. Raviraj J, Bokkasam VK, Kumar VS, Reddy US, Suman V. Radiosensitizers, radioprotectors, and radiation mitigators. Indian J Dent Res. 2014;25: 83-90.

80. Kumar S, Singh RK, Meena R. Emerging targets for radioprotection and radiosensitization in radiotherapy. Tumour Biol. 2016;37: 11589-11609.

81. Katz D, Ito E, Liu FF. On the path to seeking novel radiosensitizers. Int J Radiat Oncol Biol Phys. 2009;73: 988-996.

82. Krishnaswamy S. The transition of prothrombin to thrombin. J Thromb Haemost. 2013;11 Suppl 1: 265-276.

83. Carney DH, Herbosa GJ, Stiernberg J, et al. Double-signal hypothesis for thrombin initiation of cell proliferation. Semin Thromb Hemost. 1986;12: 231-240.

84. Glenn KC, Frost GH, Bergmann JS, Carney DH. Synthetic peptides bind to high-affinity thrombin receptors and modulate thrombin mitogenesis. Pept Res. 1988;1: 65-73.

85. Olszewska-Pazdrak B, Hart-Vantassell A, Carney DH. Thrombin peptide TP508 stimulates rapid nitric oxide production in human endothelial cells. J Vasc Res. 2010;47: 203-213.

86. Li X, Wang H, Touma E, et al. TP508 accelerates fracture repair by promoting cell growth over cell death. Biochem Biophys Res Commun. 2007;364: 187-193.

87. Vartanian KB, Chen HY, Kennedy J, et al. The non-proteolytically active thrombin peptide TP508 stimulates angiogenic sprouting. J Cell Physiol. 2006;206: 175-180.

88. Ryaby JT, Sheller MR, Levine BP, Bramlet DG, Ladd AL, Carney DH. Thrombin peptide TP508 stimulates cellular events leading to angiogenesis, revascularization, and repair of dermal and musculoskeletal tissues. J Bone Joint Surg Am. 2006;88 Suppl 3: 132-139.

89. Fossum TW, Olszewska-Pazdrak B, Mertens MM, et al. TP508 (Chrysalin) reverses endothelial dysfunction and increases perfusion and myocardial function in hearts with chronic ischemia. J Cardiovasc Pharmacol Ther. 2008;13: 214-225.

90. Norfleet AM, Bergmann JS, Carney DH. Thrombin peptide, TP508, stimulates angiogenic responses in animal models of dermal wound healing, in chick chorioallantoic membranes, and in cultured human aortic and microvascular endothelial cells. Gen Pharmacol. 2000;35: 249-254.

91. Norfleet AM, Huang Y, Sower LE, Redin WR, Fritz RR, Carney DH. Thrombin peptide TP508 accelerates closure of dermal excisions in animal tissue with surgically induced ischemia. Wound Repair Regen. 2000;8: 517-529.

92. Wang H, Li X, Tomin E, et al. Thrombin peptide (TP508) promotes fracture repair by up-regulating inflammatory mediators, early growth factors, and increasing angiogenesis. J Orthop Res. 2005;23: 671-679.

93. Wang Y, Wan C, Szoke G, Ryaby JT, Li G. Local injection of thrombin-related peptide (TP508) in PPF/PLGA microparticles-enhanced bone formation during distraction osteogenesis. J Orthop Res. 2008;26: 539-546.

94. Fife C, Mader JT, Stone J, et al. Thrombin peptide Chrysalin stimulates healing of diabetic foot ulcers in a placebo-controlled phase I/II study. Wound Repair Regen. 2007;15: 23-34.

95. Carney DH, Olszewska-Pazdrak B. Could rusalatide acetate be the future drug of choice for diabetic foot ulcers and fracture repair? Expert Opin Pharmacother. 2008;9: 2717-2726.

96. Kantara C, Moya SM, Houchen CW, et al. Novel regenerative peptide TP508 mitigates radiation-induced gastrointestinal damage by activating stem cells and preserving crypt integrity. Lab Invest. 2015;95: 1222-1233.

97. Olszewska-Pazdrak B, McVicar SD, Rayavara K, et al. Nuclear Countermeasure Activity of TP508 Linked to Restoration of Endothelial Function and Acceleration of DNA Repair. Radiat Res. 2016;186: 162-174.

98. Ajithkumar T, Price S, Horan G, Burke A, Jefferies S. Prevention of radiotherapy-induced neurocognitive dysfunction in survivors of paediatric brain tumours: the potential role of modern imaging and radiotherapy techniques. Lancet Oncol. 2017;18: e91-e100.

99. Kantara C, Moya S, Zawaski J, Gaber W, Escobar K and Carney D. TP508 Mitigates Radiotherapy-Induced Brain Tissue Damage by Stimulating the Proliferation of Neuroprogenitor Cells. . Clinical and Translational Research Forum. 2014.

100. Kantara C, O'Connell M, Sarkar S, Moya S, Ullrich R, Singh P. Curcumin promotes autophagic survival of a subset of colon cancer stem cells, which are ablated by DCLK1-siRNA. Cancer Res. 2014;74: 2487-2498.

101. Pastrana E, Silva-Vargas V, Doetsch F. Eyes wide open: a critical review of sphere-formation as an assay for stem cells. Cell Stem Cell. 2011;8: 486-498.

102. Portillo-Lara R, Alvarez MM. Enrichment of the Cancer Stem Phenotype in Sphere Cultures of Prostate Cancer Cell Lines Occurs through Activation of Developmental Pathways Mediated by the Transcriptional Regulator DeltaNp63alpha. PLoS One. 2015;10: e0130118.

103. Jensen JB, Parmar M. Strengths and limitations of the neurosphere culture system. Mol Neurobiol. 2006;34: 153-161.

104. Ivascu A, Kubbies M. Rapid generation of single-tumor spheroids for high-throughput cell function and toxicity analysis. J Biomol Screen. 2006;11: 922-932.

105. Sottoriva A, Verhoeff JJ, Borovski T, et al. Cancer stem cell tumor model reveals invasive morphology and increased phenotypical heterogeneity. Cancer Res. 2010;70: 46-56.

106. Olive PL, Banath JP. The comet assay: a method to measure DNA damage in individual cells. Nat Protoc. 2006;1: 23-29.

107. Laks DR, Masterman-Smith M, Visnyei K, et al. Neurosphere formation is an independent predictor of clinical outcome in malignant glioma. Stem Cells. 2009;27: 980-987.

108. Hardee ME, Marciscano AE, Medina-Ramirez CM, et al. Resistance of glioblastoma-initiating cells to radiation mediated by the tumor microenvironment can be abolished by inhibiting transforming growth factor-beta. Cancer Res. 2012;72: 4119-4129.

109. Ogawa K, Yoshioka Y, Isohashi F, Seo Y, Yoshida K, Yamazaki H. Radiotherapy targeting cancer stem cells: current views and future perspectives. Anticancer Res. 2013;33: 747-754.

110. Sakariassen PO, Immervoll H, Chekenya M. Cancer stem cells as mediators of treatment resistance in brain tumors: status and controversies. Neoplasia. 2007;9: 882-892.

111. Yoshida GJ, Saya H. Therapeutic strategies targeting cancer stem cells. Cancer Sci. 2016;107: 5-11.

112. Li Y, Rogoff HA, Keates S, et al. Suppression of cancer relapse and metastasis by inhibiting cancer stemness. Proc Natl Acad Sci U S A. 2015;112: 1839-1844.

113. Lagerweij T, Hiddingh L, Biesmans D, et al. A chemical screen for medulloblastoma identifies quercetin as a putative radiosensitizer. Oncotarget. 2016;7: 35776-35788.

114. Srivastava M, Raghavan Sathees C. DNA Double-Strand Break Repair Inhibitors as Cancer Therapeutics. Chemistry & Biology.22: 17-29.

115. Burma S, Chen BP, Murphy M, Kurimasa A, Chen DJ. ATM phosphorylates histone H2AX in response to DNA double-strand breaks. J Biol Chem. 2001;276: 42462-42467.

116. Kuo LJ, Yang LX. Gamma-H2AX - a novel biomarker for DNA double-strand breaks. In Vivo. 2008;22: 305-309.

117. Kuefner MA, Brand M, Engert C, Schwab SA, Uder M. Radiation Induced DNA Double-Strand Breaks in Radiology. Rofo. 2015;187: 872-878.

118. Allan AL. Cancer Stem Cells in Solid Tumors. Humana Press, 2011.

119. Taneja N, Davis M, Choy JS, et al. Histone H2AX phosphorylation as a predictor of radiosensitivity and target for radiotherapy. J Biol Chem. 2004;279: 2273-2280.

120. Thompson LH. Recognition, signaling, and repair of DNA double-strand breaks produced by ionizing radiation in mammalian cells: the molecular choreography. Mutat Res. 2012;751: 158-246.

121. McNeely S, Beckmann R, Bence Lin AK. CHEK again: revisiting the development of CHK1 inhibitors for cancer therapy. Pharmacol Ther. 2014;142: 1-10.

122. Prince EW, Balakrishnan I, Shah M, et al. Checkpoint kinase 1 expression is an adverse prognostic marker and therapeutic target in MYC-driven medulloblastoma. Oncotarget. 2016;7: 53881-53894.

123. Levesque AA, Eastman A. p53-based cancer therapies: Is defective p53 the Achilles heel of the tumor? Carcinogenesis. 2007;28: 13-20.

124. Borst GR, McLaughlin M, Kyula JN, et al. Targeted radiosensitization by the Chk1 inhibitor SAR-020106. Int J Radiat Oncol Biol Phys. 2013;85: 1110-1118.

VITA

Stephanie M. Moya was born in Miami, FL on October 19, 1989 to Salomon and Digna Moya. Stephanie graduated from Homestead Senior High School in 2008 as Valedictorian and recipient of the Gates Millennium Scholarship. During her high school training she also completed a licensed practical nursing program. In 2012, she graduated from the University of Miami with a Bachelor of Science degree in Microbiology and Immunology with minors in Chemistry and Psychology.

Stephanie joined the University of Texas Medical Branch in 2012 as a PREP (post-baccalaureate research program) student and was later admitted as a graduate student and Presidential Scholar in the Biochemistry and Molecular Biology program in 2013. During her graduate training she was involved in various organizations in the university, including co-chairing the Committee for Career Development and the Biological Chemistry Student Organization. She mentored and/or trained three PREP students, one high school Bench program student, and one medical student. She also taught as a student facilitator in the graduate school introductory biochemistry course. Additionally, Stephanie served as a student representative on both the Basic Biomedical Science Curriculum and Biochemistry and Molecular Biology curriculum committees.

During her time at UTMB Stephanie was awarded several scholarships and awards, including the Who's Who Among Students in American Universities and Colleges, the Best Poster Presentation in Pharmacology & Toxicology at the National Student Research Forum, and the Betty J. Williams Scholarship for academic excellence. Over the course of her career she has received 16 academic awards, submitted a total of 7 abstracts, presented 8 poster presentations, and co-authored one patent and three publications.

This dissertation was typed by Stephanie Michelle Moya

PUBLICATIONS

1. Olszewska-Pazdrak B., McVicar S., Rayavara K., **Moya S.**, Kantara C., Gammarano C., Olszewska P., Fuller G., Sower L. and Carney D. Nuclear Countermeasure Activity of TP508 Linked to Restoration of Endothelial Function and Acceleration of DNA Repair. *Radiation Research*, Aug 2016, 186:162-174.

2. Kantara C., **Moya S.**, Houchen C., Umar S., Singh P. and Carney D. Novel regenerative peptide TP508 mitigates radiation-induced gastrointestinal damage by activating stem cells and preserving crypt integrity. *Laboratory Investigation*, Aug 2015, doi: 10.1038/labinvest.2015.103.

3. Kantara C., O'Connell M., Sarkar S., **Moya S.**, Ullrich R. and Singh P. Curcumin Promotes Autophagic Survival of a Sub-Set of Colon Cancer Stem Cells, which are Ablated by DCLK1-siRNA. *Cancer Research*, May 2014, 74:2487-2498.

ABSTRACTS

1. Moya S., Kantara C., Sower L., and Carney D. TP508 sensitizes cancer stem cells to radiation and delays brain cancer cell relapse *in vitro.* Proceedings of the 106th Annual Meeting of the American Association of Cancer Research Meeting. April 2015, Philadelphia, PA. Abstract# 3341. Cancer Research: August 1, 2015; Vol. 75, Supplement 15.

2. Moya S., Kantara C., Zhong M., Sower L., and Carney D. TP508 peptide prevents brain tumor relapse by sensitizing cancer stem cells to radiation therapy. The 60th Annual

Meeting of the Radiation Research Society. September 24, 2014 Las Vegas, NV. Abstract# 796.

3. Kantara C., **Moya S**., Singh P., Houchen C. and Carney D. TP508, a novel peptide, prevents radiation-induced damage to colonic crypts by rescuing loss of stemness and stimulating proliferation. The 60th Annual Meeting of the Radiation Research Society. September 24, 2014 Las Vegas, NV. Abstract# 765.

4. Kantara C., **Moya S.**, Zawaski J., Gaber M. and Carney D. TP508 Mitigates Radiotherapy-Induced Brain Tissue Damage by Stimulating the Proliferation of Neuroprogenitor Cells. The 2013 Annual American Society for Cell Biology Meeting. December, 2013 New Orleans, LA. Mol. Biol. Cell. Vol 24, Issue 24, Page 4207. Abstract# 864.

5. Kantara C.**, Moya S.**, Fant C., Bremer J. and Niesel D. The Committee for Career Development: A Collaborative Group Promoting the Careers and Development of Students and Fellows. Presented at the 2013 GREAT Group Annual Professional Development Conference. Sept 19th, 2013 Atlanta GA.

6. Sarkar S., O'Connell M., **Moya S.**, and Singh P. Opposite effects of curcumin on the expression of short (S) form of stem-cell-marker, DCLK1, in non-transformed vs. transformed cells, resulting in either stabilization or inhibition of cell proliferation, respectively. Proceedings of the Digestive Disease Week, May 18-21 2013. Gastroenterology Vol. 144, Issue 5, Supplement 1, Page 596.

7. Sarkar S., O'Connell M., **Moya S.**, and P. Singh. Curcumin either stimulates or inhibits expression of short isoform of stem-cell-marker DCLK1 (DCLK1-S) in non-transformed

vs transformed cells, resulting in stabilization/inhibition of growth, respectively. Proceedings of the 104th American Association of Cancer Research Meeting, April 6-10, 2013. Abstract #2574. Cancer Research: April 15, 2013; Vol. 73, Supplement 8.

PATENT

1. Kantara, C., Carney C., **Moya S.** (Co-inventor). "Methods of Using Thrombin Derivatives to Treat Cancer". Provisional Patent. Filed on June 11th, 2014 by David L. Provence on behalf of UTMB. Confirmation #8977.